NASA Technical Memorandum 4058

Concept Development of a Mach 3.0 High-Speed Civil Transport

A. Warner Robins
Planning Research Corporation
Hampton, Virginia

Samuel M. Dollyhigh
Langley Research Center
Hampton, Virginia

Fred L. Beissner, Jr., Karl Geiselhart, Glenn L. Martin,
E. W. Shields, and E. E. Swanson
Planning Research Corporation
Hampton, Virginia

Peter G. Coen and Shelby J. Morris, Jr.
Langley Research Center
Hampton, Virginia

National Aeronautics
and Space Administration

**Scientific and Technical
Information Division**

1988

Summary

A baseline Mach 3.0 high-speed civil transport concept was developed as part of a national program with the goal that concepts and technologies be developed that will enable an effective long-range high-speed civil transport system. The Mach 3.0 airplane concept reported herein represents an aggressive application of advanced technologies to achieve the design goals. The level of technology is generally considered to be that which could have a demonstrated availability date of 1995–2000. The results indicate that aircraft are technically feasible that could carry 250 passengers at Mach 3.0 cruise for a 6500-n.mi. range at a size, weight, and performance level that allow it to fit into the existing world airport structure. The details of the configuration development, aerodynamic design, propulsion system and integration, mass properties, mission performance, and sizing are presented.

Introduction

Recent and projected trends in world travel indicate that travel to the Pacific Basin nations will increase at a rate of more than three times that of travel on the North Atlantic routes. Currently, the subsonic airplanes flying these long-range routes have a travel time of 12 to 14 hr. As travel and trade with the Pacific Basin countries increase, the demand will increase for more productive forms of air travel. Substantial reduction of flying time results in a large reduction in human fatigue and improved effectiveness at the destination. A study by the Office of Science and Technology Policy, Executive Office of the President (ref. 1) identified the technology development to support a long-range supersonic transport as one of three national goals and recommended that the American aeronautics community direct its skills and energies toward these high-payoff national goals to sustain the nation's leadership position in aeronautics. It further recommended that industry and NASA determine the most attractive technical concepts and the necessary technology developments for future long-range high-speed civil transports. NASA, in keeping with its charter, has conducted research on a continuing basis that is applicable to sustained supersonic cruise airplanes. In response to the Office of Science and Technology Policy recommendations, NASA has conducted technology integration studies focused at investigating long-range high-speed civil transport feasibility and technology requirements.

Analysis of the worldwide airline route structure indicated that an airplane with a range slightly in excess of 6000 n.mi. would be capable of flying 90 percent of the long-range market routes. This fact and an examination of some major international city pairs led to establishing a 6500 n.mi. range as a goal for high-speed civil transport studies. Further preliminary studies indicated that block time (the time required to go from the departure gate to the arrival gate) plotted against cruise Mach number has a "knee" in the curve at Mach 3.0 to 5.0 for the 6500 n.mi. range. Block times at Mach numbers above these are increasingly dominated by the time spent in acceleration, deceleration, and ground operations. The subject of this report is a Mach 3.0 concept used to determine the feasibility of the design goals and is to be used as a baseline for examining emerging technologies to identify and assess those that will enable an effective long-range high-speed civil transport system. Mach 3.0 was not chosen as a design Mach number as a result of a market utility analysis, but because it is believed to represent approximately the upper Mach number limit for simple thermal management systems. Higher cruise Mach numbers lead to the requirement for large amounts of insulation and/or no fuel carried in the wing at cruise and finally to the requirement for an active cooling system. Other baseline concepts will examine the feasibility and technology required to push further into the Mach 3.0 to 5.0 range that is of interest for high-speed civil transports.

The Mach 3.0 concept reported herein represents an aggressive application of advanced technology to achieve the design goals. The level of technology is generally considered to be that which could have a demonstrated availability date of 1995–2000. The concept serves as a baseline for the renewed studies into high-speed commercial transportation and serves to indicate the technical feasibility of such an aircraft. Current studies of high-speed transportation systems entertain the concept of "super hubs" from which high-speed civil transports could operate with modifications of current noise constraints. The concept reported herein has no noise constraints on the aircraft and engine performance. The reader should be aware that meeting current noise requirements will most probably result in a larger takeoff gross weight than indicated. Even so, the intent of the report is still met in that the concept serves as a baseline from which to assess the overall effects of meeting additional requirements such as sideline noise or sonic boom overpressure limits.

The design, development, and analysis of a Mach 3.0 civil transport are presented in this paper. The concept was sized to carry 250 passengers for 6500 n.mi. with reserves. Advanced propulsion, structures, controls, and aerodynamics are employed in the concept. Several design features of the concept would require challenging technology development programs to meet the projected technology availability date. Details of the design development, aerodynamic design, propulsion system and integration, mass properties, sizing, and mission performance are presented.

Symbols

A_o	inlet area, ft^2
A_x	average equivalent body cross-sectional area, ft^2
b	wing span, ft
C_D	drag coefficient, D/qS
C_L	lift coefficient, L/qS
C_m	pitching-moment coefficient, Pitching moment$/qS\bar{c}$
C_μ	thrust coefficient, T/qS
c	local airfoil chord, ft
$\bar{c}$	mean aerodynamic chord, ft
D	drag, lb
g	acceleration due to gravity
h	altitude, ft
L	lift, lb
M	Mach number
m	mass flow, lb/sec
m_o	mass flow at inlet, lb/sec
q	dynamic pressure, lb/ft^2
S	reference area, ft^2
S_s	leading-edge suction parameter
T	thrust, lb
$T_i; i = 1, 2, 3, 4$	trailing-edge flap designation
t	airfoil thickness, ft
V	airspeed, KCAS
W	weight, lb
w_N	width of nozzle, ft
x	longitudinal distance along fuselage from nose, ft
x_N	distance from wing trailing edge to nozzle exit plane, ft
α	angle of attack, deg
β	Prandtl-Glauert compressibility correction factor $(M^2 - 1)^{1/2}$
Δ	increment
δ	deflection angle, deg
Λ_o	Mach angle, deg

Subscripts:

b	base
DES	design
f	friction
form	form
i	induced
max	maximum
N	nozzle
o	zero lift
R	roughness
slot	slot
TE	trailing edge
v	thrust vector
w	wave
Γ	circulation
∞	free stream

Abbreviations:

Alt	altitude, ft
ATA	Air Transport Association
c.g.	center of gravity
DGW	design gross weight, lb
EW	empty weight, lb
FS	fuselage station, in.
KCAS	knots calibrated airspeed
LE	leading edge
LET	leading-edge thrust
MAC	mean aerodynamic chord, ft
MRT	military rated thrust, lb
OW	operating weight, lb
OWE	operating weight empty, lb
SFC	specific fuel consumption, $\frac{\text{lb/hr}}{\text{lb}}$

SREF	reference area, ft^2
TDF	time, distance, and fuel
WL	water line, in.
ZFW	zero-fuel weight, lb

Design Concept and Description

The baseline concept, illustrated in figure 1, is a blended wing-body configuration with a modified platypus nose, a highly swept inboard wing panel, a moderately swept outboard wing panel, and curved wingtips. The wing planform was selected to minimize induced drag (inversely proportional to span squared) and wave drag due to lift (inversely proportional to lifting length squared) while maintaining adequate low-speed characteristics. A basic delta planform can be progressively modified, as shown in figure 2, to have substantially less area and consequently less weight and friction drag at little expense in drag due to lift if span loading and length loading are maintained. Further, the compound-leading-edge planform can provide, as in the case of the Anglo-French Concorde, a minimum shift in the aerodynamic center between takeoff and supersonic cruise speeds. Additionally, with adequate wing twist, the lifting forewing can provide large favorable flap-trimming pitching moments. Nose blunting, either by volume or by lift, can significantly reduce the maximum sonic boom overpressure (ref. 2). The advantage of lift blunting, the Mach equivalent volume associated with the lift which is produced by a platypus nose, over configuration volume blunting is that zero-lift wave drag is not affected. Lift blunting can also produce high initial upwash in which the remainder of the wing might fly for improved drag at lift.

The inboard wing panel is swept 79°, allowing the Mach number normal to the leading edge to be subsonic even at the Mach 3.0 cruise condition. The high sweep also allows blunt leading edges without a wave-drag penalty. The low Mach number normal to the leading edge and the leading-edge bluntness result in an insensitivity of optimum leading-edge camber to flight speed and section performance to wing camber, thus allowing the inboard leading edge to have fixed geometry, i.e., no leading-edge flap, actuators, or resisting structure. This results in a lighter and less complex wing.

The outboard wing panel is swept 53° with a curved tip. At low speeds and high angle of attack, flow separation at the wingtip is common, and for highly swept wings tends to produce a severe pitch-up. A highly curved wingtip with controlled vortex separation, as shown in figure 3, tends to relieve this pitch-up (ref. 3). The trailing-edge extension at the tip is additional surface on which the well-developed upper-surface vortex might operate to generate suction or lift. Other investigators have found (refs. 4, 5, and 6) that wings with curved tips also have substantially better induced drag characteristics. The leading-edge notch flap is a low-speed device aimed at retaining potential flow on the outboard panel while the flow inboard remains unavoidably three-dimensional. With the notch flap down (fig. 4), there is not only a much more pronounced separating notch, but the deflected notch flap functions as a leading-edge pylon vortex generator (ref. 7). The vortex flow that is produced by the deflected notch flap rotates in a direction opposite to that of the vortex shed by the inboard wing panel. This tends to decrease the upwash on the outboard wing panel and thus allows the flow to remain attached over a larger angle-of-attack range. This in turn delays pitch-up, allowing more lift to be developed, and thus decreases approach speed. Preliminary results from a water tunnel test confirm the operation of the notch flap (fig. 5).

The high-lift devices incorporated into the design, in addition to the leading-edge notch, are 15 percent chord leading-edge flaps on the outboard panel, 25 percent chord trailing-edge flaps, and deflected engine nozzles. The nozzles on the configuration are set at 5° downward deflection (consistent with vehicle trim) to provide that the gross thrust vector develops not only a lift vector component but some supercirculation as well.

Because of aerodynamic considerations, the forebody of the concept is very slender. This causes the flight crew to be located 44 ft aft of the nose. The long forebody and the span of the forewing at the crew station prevent normal vision requirements to be met without a variable-geometry forebody; however, a variable-geometry platypus nose would provide insurmountable adverse longitudinal trim properties and also have a large weight penalty. A see-by-wire system in which multiple planar visual displays, similar to flight simulator scene-generation displays, was therefore chosen in lieu of windows. Such a system could provide for variable gain in both the visible and nonvisible spectra (e.g., radar and infrared), enhancing visibility and safety at night and in adverse weather. In addition to the improved visibility available in flight, ground handling visibility should be much improved with the multiple camera locations available. The flight station has provision for the pilot and copilot in a side-by-side arrangement with a jump seat for an observer if needed. The avionics and electronics racks are located aft of the flight station, thereby affording easy access for maintenance and systems servicing. The main cabin section is configured for 250 passengers at 3 to 6 abreast seating with 34 in. pitch. Six lavatories are provided, with 2 forward, 2 amidships, and 2 in the aft cabin. One main entrance door is located on each side of the fuselage between the aft lavatory and galley. These doors are also used to service the galley. In addition, 6 emergency exits are provided for over-the-wing egress. Like the cockpit, the cabin is windowless. This simplifies the problem of cabin structural design and environmental control as exterior skin temperatures approach 550°F in cruise. Outside visibility and entertainment for the passengers would be provided by individual video systems mounted on seat backs similar to those now under commercial development.

The main landing gear is a three-strut arrangement with six wheels per strut. Two struts are wing mounted and retract inboard into the fuselage below the cabin floor. A centerline strut is fuselage mounted and retracts forward. The nose gear has two wheels and is mounted on the forward bulkhead of the flight station and retracts forward. Each gear strut is a dual-acting hydraulic cylinder with one action for landing shock and the second for strut compression to facilitate easier gear stowage.

Six engines are mounted in two nacelles on the wing lower surface adjacent to the fuselage. This allows the engine mounting structure to utilize the fuselage structure to increase stiffness and improve flutter boundaries. The inlet is located so as to use wing/fuselage precompression to lower the inlet Mach number and thus reduce the inlet size. The longitudinal location of the inlet/nacelle is such as to provide for favorable lift and drag interference between the nacelle and the wing lower surface. The inlets themselves are mixed compression (some internal contraction and therefore variable geometry) in the interest of retaining high-pressure recoveries without high external drag. The boundary-layer diverter for the outside engines directs the low-energy boundary-layer flow to the outside of the engines in a normal manner while the boundary layer ahead of the center inlet is diverted through the wing aft of the rear spar. With the engines located adjacent to each other in the pods, an active unstart control system would be required in order to prevent an engine unstart from affecting adjacent engines. Remote gearbox and accessories are mounted in the fuselage below the cabin floor between the wing rear spar carry-through and the aft fuselage fuel tank and are driven by engine extension shafting.

Fuel is contained in 34 integral wing tanks and 3 aft fuselage tanks. The aft fuselage tanks are used primarily for aircraft center-of-gravity control. The subsystems, which include environmental control, hydraulics, electrical, and auxiliary power, are mounted below the cabin floor aft of the rear spar carry-through.

Because of the elliptical forebody cross section, directional stability at high angles of attack improves (ref. 8), where more conventional wing/fuselages degrade sharply. Thus the directional surface is largely rudder and is sized by engine-out conditions. The requirement for a large vertical tail is greatly relieved by the canted nozzles being set close to the aircraft centerline. Figure 6 is an interior arrangement drawing of the concept showing the location of the above items. Table I presents the geometric characteristics of the concept.

Mass Properties

An estimation of the aircraft weight and balance, shown in table II and figure 7, is derived from an empirically based transport weight analysis computer program. The formulas were developed from a data base of current transport aircraft with structures and subsystems weights based on conventional aluminum and titanium construction. Each formula has incorporated a technology factor to account for improvements in manufacturing or materials that will reflect weight reduction.

For this study, several areas of technology improvements have been assumed. The fuselage is constructed primarily of superplastic-formed and diffusion-bonded titanium. Wing structure including fairings, control surfaces, and fuel tanks are predominately made of composite material such as graphite or Kevlar[1] and polyimide. For the landing gear, radial ply tires with lightweight forged wheels and carbon brakes are used. The hydraulic system weight is based on a 5000 psi operating pressure with titanium lines and fittings. For the remaining subsystems such as electrical, instruments, auxiliary power, environmental control, and avionics, a technology improvement of 15 to 20 percent over current systems has been assumed.

Aerodynamics

Zero-lift drag. The buildup of zero-lift drag for the clean configuration is shown as a function of Mach number in figure 8. The values shown are those corresponding to an altitude of 40 000 ft. Skin-friction drag values were calculated by the T' method

[1] Kevlar: Registered trademark of E. I. du Pont de Nemours & Co., Inc.

of Sommer and Short (ref. 9). Form drag was calculated by the subsequent application of geometry-dependent factors of reference 10, and roughness drag was estimated from empirical data. The slot drag increment accounts for the drag of the center inlet boundary-layer bleed slot and is based on mass flow considerations. Wave-drag evaluation was accomplished by a method based on reference 11. The numerical model in the form described in reference 12 is provided in table III with a plot of the data shown in figure 9. One feature of the program for wave-drag evaluation is an ability to define a minimum-wave-drag fuselage area distribution through a set of constraining fuselage stations in a given assemblage of aircraft components at a given Mach number. This feature was used to define the fuselage cross-section-area distribution at the design Mach number of 3.0. The resulting Mach 3.0, average-equivalent-body buildup is shown in figure 10.

Lift-dependent drag. Supersonic lift-dependent drag, as well as angle of attack and static longitudinal stability characteristics, was evaluated by the modified linear-theory method of references 13 through 16. The wing design methods used also came from this series of documents. The numerical model generated and used is in the format of reference 12 and is listed in table IV, and a configuration plot is shown in figure 11. Since this is used with a lifting surface code, the aft section of the fuselage was not included in the model. Figure 12 shows lift-dependent drag at a start cruise point ($M = 3.0$ and 65 670 ft). Note that the final supersonic drag values differ from the no-leading-edge-thrust polar by several increments, one of which contains not only the leading-edge thrust attainable, but that portion that manifests itself as vortex lift (see ref. 17). Another major increment is that due to camber and twist. Noted on the figure as well is an increment due to the 5° turn of the internal flow by the nacelle prior to nozzle entry. This latter increment is in place of any consideration of the external lift and drag effects of this down-turn of the flow over the portion of the total planform covered by the nacelle/nozzle combination. Any lift on the wing induced by deflected nozzle flow (supercirculation) was not accounted for at supersonic speeds. The typical supersonic total-drag polars for Mach numbers 1.4, 2.2, and 3.0 are shown in figure 13.

Subsonic lift-dependent drags were generated by the method of reference 17, which accounts for the effects of leading-edge thrust and/or vortex lift. This method was also used to establish the flap scheduling for the mission-adaptive wing and the associated envelope polars used in performance analysis. The data as developed by the method of reference 17 were modified to include the effect of the 5° nacelle/nozzle bend as well as supercirculation (but not direct gross-thrust-vector effects). A typical drag polar buildup, with the equations used to develop these latter values, is shown for Mach number 0.6 in figure 14.

To illustrate the more demanding case in which not only are thrust level and the attendant noise critical, but consideration of scrape angle and trimming capability is vitally important, figures 15 through 17 address the problem of idealizing wing geometry for takeoff at maximum takeoff weight. In these figures, it is assumed that gross-thrust coefficient is a constant corresponding to six-engine, military-rated thrust (MRT), not a variable as shown in figure 14 where net thrust equals drag and gross thrust is assumed twice the net thrust. Figure 15 is a typical flap-optimization chart covering lift coefficients of 0.2, 0.4, and 0.6 at the flight conditions of $M = 0.3$ and sea level. Shown are contours of constant S_s (leading-edge-suction parameter), angle of attack, and pitching-moment coefficients (reference center at $x = 160$ ft) for various leading- and trailing-edge flap deflections (expressed here in terms of the ratio of the tangents of flap deflection angle to the tangents of the input flap deflections). The flap deflections for peak S_s values (or least drag due to lift) are called out for each lift coefficient. It is to be noted that for all those design lift coefficients, the most out-of-trim condition at peak S_s corresponds to less than one quarter of the available center-of-gravity control. To be noted as well is that scrape angle is not reached until lift coefficients beyond 0.6 are developed.

Figure 16 shows the schedule of optimum flap settings as a function of lift coefficient, based on figure 15. Note that the trailing-edge flap settings are modest, leaving substantial flap travel for control purposes. Figure 17 presents induced drag polars for the no-flap-deflection case and for the three design lift coefficients shown in figure 15. The mission-adaptive wing polar is seen to be the envelope of these polars.

Representative polars for other subsonic Mach numbers are shown in figure 18. Those for Mach numbers 0.6 and 0.9 have not been subject to as rigorous analysis as that illustrated for the Mach 0.3 case, but should be adequate for the purposes of this study.

Maximum lift-drag ratio. A plot of trimmed maximum lift-drag ratio versus Mach number is shown in figure 19. The zero-lift drags used in the generation of these values correspond to an altitude of 40 000 ft. Maximum values vary from about 14.0 at high subsonic speeds to 9.4 at Mach 3.0.

Stability considerations. Figure 20 shows aerodynamic-center shift with speed. A peculiarity of the wing planform is that the low speed and supersonic cruise points are virtually coincident. The rapid forward movement with increasing supersonic speed is probably associated with an increasing lift-curve slope of the forward portion of the wing as its leading edge becomes more nearly sonic, while that of the aft, supersonic-leading-edge section of the wing remains essentially constant. The large aft shift of aerodynamic center in the transonic range is well within the range of trim provided by the previously presented center-of-gravity envelope, even without the very large and favorable positive zero-lift pitching moments provided by the "lifting platypus forebody" section of the planform.

The extent to which center of gravity may be moved aft for trim in supersonic cruise configurations is often dependent on the level of directional stability available. Although there is evidence that the present configuration has ample directional stability throughout its speed range (see fig. 20 of ref. 18, and note the differences in directional surface requirements between the fully straked Lockheed YF-12C aircraft and the unstraked Lockheed YF-12A aircraft), it is sufficiently important to concept development that it should be demonstrated early in the program.

Propulsion

The propulsion system used for this study is a scaled version of the GE21/J11-B14a, an augmented (afterburning), double-bypass variable-cycle engine that was used in the study summarized in reference 19. The engine data in this reference were modified to reflect 1995 technology readiness and were extrapolated to cover the required Mach 3.0 cruise of the present study. The engine has a design overall pressure ratio of 13.5 and a bypass ratio of 0.25. It develops 61 271 lb of net thrust at sea level static maximum augmented power conditions. Uninstalled weight of the baseline engine is estimated to be 8042 lb, which includes the nozzle and the thrust reverser. The engine geometry is shown in figure 21. The installed performance of the baseline engine is summarized in figures 22 and 23 and table V.

The inlet data of reference 20 were used to furnish the installation penalties. The engine performance data were adjusted for the effects of inlet pressure recovery, service bleed, and power extraction as well as afterbody, inlet spillage, and bypass drags. Nacelle geometric data were developed in order to estimate nacelle drag and weight for the above inlet and engine combination.

Performance and Sizing

This section presents an estimate of the performance capabilities of the baseline concept and the results of sizing the wing area and engine size for minimum takeoff gross weight to accomplish the mission. It should be noted that detailed calculations are used for some of the fuel allowances rather than the traditional method of using fixed time operations at certain engine power levels. The 6500 n.mi. design range (no wind) can be achieved at a ramp weight of 713 696 lb including reserves as determined using the Flight Optimization System (FLOPS) computer program of reference 21.

The design mission (table VI and fig. 24) includes:

A. Fuel for 10 minutes at idle power for warm-up and taxi out.
B. Fuel for actual performance of the takeoff maneuver to the start of climb condition (at maximum afterburner power).
C. Time, distance, and fuel (TDF) for the actual climb (minimum fuel to climb path). Meets the FAA requirements of $V \leq 250$ KCAS, $h \leq 10\,000$ ft, and an arbitrary dynamic pressure limit of 1000 psf. Power setting in the climb varies from maximum nonafterburner to maximum power.
D. TDF for cruise at best altitude ($h \leq 70\,000$ ft) at $M = 3.0$.
E. TDF for actual descent at maximum L/D, zero thrust, idle fuel flow as per table V.
F. Reserve fuel allowance (no range credit) as per table VII.

    1. Perform missed approach using estimated fuel to accelerate from power-off stall speed to beginning of reserve climb path ($M = 0.3$, h = 0) at maximum afterburner thrust (at actual end-of-trip weight).
    2. Climb to reserve cruise condition.
    3. Cruise at best subsonic Mach number and altitude. Required distance to alternate airport is 250 n.mi., including climb and descent.
    4. Hold for 30 minutes at Mach number and altitude for minimum fuel flow (no range credit).
    5. Actual descent from hold condition at maximum L/D ratio, zero thrust.
    6. Additional fuel reserve allowance: 5 percent of trip fuel (C, D, and E above).

G. No time, fuel, or distance credit or penalty for approach, landing, or taxi in.

The climb and descent profiles are shown in figure 25. Factors that are not included, but could have a substantial effect on the climb paths, include sonic boom, flyable airspeed or Mach number, and resulting normal or longitudinal g forces.

Figure 26 presents the sensitivity data for the baseline aircraft weight summary of table II that were used in sizing the propulsion system and wing area to determine the minimum takeoff gross weight that meets the mission requirements.

Figure 27 shows a "thumbprint" design chart for the baseline concept. The thumbprint consists of contours of constant takeoff gross weight imposed on a grid of aircraft wing loading and thrust-weight ratio. All the potential configurations represented in the figure meet the design mission range of 6500 n.mi. Also shown on the figure are curves that represent specific values for some of the important design constraints. These constraints include takeoff field length (one engine out), approach speed, and minimum climb thrust margin. Climb thrust margin is defined as

$$\frac{\text{Max thrust}}{\text{Drag}} - 1$$

and is a parameter used to indicate the amount of thrust available over and above the thrust required to perform the climb.

The constraint lines delimit designs that are feasible under specified performance requirements and can be used to determine the minimum gross weight required to perform the design mission. In this case, an aircraft with a wing loading of 77 psf and thrust-weight ratio of 0.30 would have a minimum takeoff gross weight of 620 000 lb under the constraints of a 10 000-ft takeoff field length and a 150-knot approach speed.

Although the information provided by the thumbprint provides an engine size and a wing size to minimize weight for the required mission, a configuration redesign and rebalance is necessary to achieve such performance. A highly blended and integrated configuration such as the subject of this report requires a great deal of care in the sizing to maintain the desired configuration attributes. Another implication of the reduced takeoff gross weight is the possibility of reducing the number of engines from six to four. Six engines were originally used in anticipation that very heavy vehicles would be required for the long range.

Figure 28 illustrates the effect of design range requirement on the takeoff gross weight for an aircraft with a wing loading of 85 psf and a thrust-weight ratio of 0.35. This combination was selected because it is in the region of minimum gross weight. The design mission range of 6500 n.mi. falls well below the knee of the curve. This indicates that the range requirement is not driving the configuration to an excessively high weight. This curve is sensitive to aerodynamic, structural, and propulsive efficiencies, but the fact that the 6500 n.mi. range lies in the flat part of the curve indicates that the efficiencies could be underestimated or environmental constraints, such as noise or sonic boom, imposed without the airplane concept becoming excessively heavy.

Concluding Remarks

A baseline Mach 3.0 high-speed civil transport concept was developed as part of a national program with the goal that concepts and technologies be developed that will enable an effective long-range high-speed civil transport system. The details of the configuration development, aerodynamic design, propulsion system and integration, mass properties mission performance, and sizing were presented.

The concept is configured to carry 250 passengers at 3 to 6 abreast seating for 6500 n.mi. with reserves. The concept is highly integrated and blended to achieve efficient volume utilization and high aerodynamic efficiency. The wing planform is tailored to minimize supersonic drag due to lift and wave drag while maintaining good low-speed characteristics. Particular attention is paid to the incorporation of high lift and vortex control devices to overcome aerodynamic deficiencies associated with highly swept wing planforms at low speeds. Maximum trimmed lift-drag ratios vary from 14.0 at high subsonic speed to 9.4 at Mach 3.0.

Six advanced variable-cycle turbojet engines are mounted in two nacelle packages on the lower surface of the wing adjacent to the fuselage. Six engines were used in anticipation that very heavy vehicles would be required for the long range. The mixed compression inlets are located so as to take advantage of wing/fuselage precompression. The engine data used was based on an augmented, double-bypass variable cycle engine concept that was developed as part of a previous supersonic cruise program. The data were modified to reflect an advanced 1995 technology readiness and were extrapolated from Mach 2.7 to 3.0 to cover the Mach 3.0 cruise of the present study.

Advanced but not exotic materials, structures, and subsystems are used. Superplastic-formed and diffusion-bonded titanium is used for fuselage structure and composites are used for wing and fuel tank structure. Subsystem weight is reduced 15 to 20 percent from current systems to account for technology improvements. The baseline aircraft capable of meeting the range and performance requirements was estimated to weigh 713 696 lb. An aircraft of this size and weight is considered to be an acceptable candidate to fit into the existing world airport infrastructure.

The baseline concept was further studied by conducting a sizing exercise to determine the engine size and wing area that result in minimum takeoff gross weight and meet the performance requirements. Sizing the baseline concept to a wing loading of 77 psf and a thrust-weight ratio of 0.30 would result in a takeoff gross weight of approximately 620 000 lb. The takeoff field length (10 000 ft) and the approach speed (150 knots) are the two most stringent requirements that determine the minimum takeoff gross weight. The concept reported has no noise constraints on the aircraft and engine performance, so meeting this requirement will result in a larger takeoff gross weight than indicated. However, the baseline concept serves as a departure point from which to assess the overall effects of meeting additional requirements as well as the positive benefits of incorporating emerging advanced technologies.

NASA Langley Research Center
Hampton, VA 23665-5225
August 2, 1988

References

1. *National Aeronautical R & D Goals—Agenda for Achievement.* Executive Off. of the President, Off. of Science & Technology Policy, Feb. 1987.
2. Carlson, Harry W.: Influence of Airplane Configuration on Sonic-Boom Characteristics. *J. Aircr.*, vol. 1, no. 2, Mar.–Apr. 1964, pp. 82-86.
3. van Dam, C. P.: Swept Wing-Tip Shapes for Low-Speed Airplanes. *SAE Trans.*, Sect. 6, vol. 94, 1985, pp. 6.355–6.364.
4. van Dam, C. P.: Induced-Drag Characteristics of Crescent-Moon-Shaped Wings. *J. Aircr.*, vol. 24, no. 2, Feb. 1987, pp. 115–119.
5. Vijgen, P. M. H. W.; van Dam, C. P.; and Holmes, B. J.: Sheared Wing-Tip Aerodynamics: Wind-Tunnel and Computational Investigations of Induced-Drag Reduction. AIAA-87-2481 CP, Aug. 1987.
6. Naik, D. A.; and Ostowari, C.: An Experimental Study of the Aerodynamic Characteristics of Planar and Non-Planar Outboard Wing Planforms. AIAA-87-0588, Jan. 1987.
7. Rao, Dhanvada M.; and Johnson, Thomas D., Jr.: *Subsonic Pitch-Up Alleviation on a 74 Deg. Delta Wing.* NASA CR-165749, 1981.
8. Brandon, Jay M.; Murri, Daniel G.; and Nguyen, Luat T.: Experimental Study of Effects of Forebody Geometry on High Angle of Attack Static and Dynamic Stability and Control. *ICAS Proceedings—1986, 15th Congress of the International Council of the Aeronautical Sciences, Volume 1,* P. Santini and R. Staufenbiel, eds., American Inst. of Aeronautics and Astronautics, Inc., 1986, pp. 560–572. (Available as ICAS-86-5.4.1.)
9. Sommer, Simon C.; and Short, Barbara J.: *Free-Flight Measurement of Turbulent-Boundary-Layer Skin Friction in the Presence of Severe Aerodynamic Heating at Mach Numbers From 2.8 to 7.0.* NACA TN 3391, 1955.
10. *USAF Stability and Control Datcom.* Contracts AF33(616)-6460 and F33615-76-C-3061, McDonnell Douglas Corp., Oct. 1960. (Revis. Apr. 1978.)
11. Harris, Roy V., Jr.: *An Analysis and Correlation of Aircraft Wave Drag.* NASA TM X-947, 1964.
12. Craidon, Charlotte B.: *Description of a Digital Computer Program for Airplane Configuration Plots.* NASA TM X-2074, 1970.
13. Middleton, W. D.; and Lundry, J. L.: *A System for Aerodynamic Design and Analysis of Supersonic Aircraft. Part 1—General Description and Theoretical Development.* NASA CR-3351, 1980.
14. Middleton, W. D.; Lundry, J. L.; and Coleman, R. G.: *A System for Aerodynamic Design and Analysis of Supersonic Aircraft. Part 2 - User's Manual.* NASA CR-3352, 1980.
15. Middleton, W. D.; and Lundry, J. L.: *A System for Aerodynamic Design and Analysis of Supersonic Aircraft. Part 4—Test Cases.* NASA CR-3354, 1980.
16. Carlson, Harry W.; Mack, Robert J.; and Barger, Raymond L.: *Estimation of Attainable Leading-Edge Thrust for Wings at Subsonic and Supersonic Speeds.* NASA TP-1500, 1979.
17. Carlson, Harry W.; and Walkley, Kenneth B.: *An Aerodynamic Analysis Computer Program and Design Notes for Low-Speed Wing Flap Systems.* NASA CR-3675, 1983.
18. Parlett, Lysle P.; and Shivers, James P.: *Low-Speed Wind-Tunnel Tests of a Large-Scale Blended-Arrow Advanced Supersonic Transport Model Having Variable-Cycle Engines and Vectoring Exhaust Nozzles.* NASA TM X-72809, 1976.
19. Walkley, K. B.; Espil, G. J.; Lovell, W. A.; Martin, G. L.; and Swanson, E. E.: *Concept Development of a Mach 2.7 Advanced Technology Transport Employing Wing-Fuselage Blending.* NASA CR-165739, 1981.
20. Koncsek, J. L.; and Syberg, J.: *Transonic and Supersonic Test of a Mach 2.65 Mixed-Compression Axisymmetric Intake.* NASA CR-1977, 1972.
21. McCullers, L. A.: Aircraft Configuration Optimization Including Optimized Flight Profiles. *Recent Experiences in Multidisciplinary Analysis and Optimization,* Jaroslow Sobieski, compiler, NASA CP-2327, Part 1, 1984, pp. 395-412.

Table I. Configuration Geometry

Geometry	Wing	Vertical
Area, ft^2	12 185	131.6
MAC, ft	129.65	18.92
Span, ft	150.0	8.0
Aspect ratio	3.039	0.486
Taper ratio		0.196
LE sweep, deg	79.56, 53.13	70.10
Root chord, ft		27.50
Tip chord, ft		5.40
Root t/c, percent		2.500
Tip t/c, percent		2.500
Volume coefficient		0.012

Table II. Estimated Weights and Balance

Item	Weight, lb	FS c.g., in.	WL c.g., in.
Wing	56 258	2050.0	85.0
Horizontal	0		
Vertical	1 101	3462.4	297.3
Fin	0		
Canard	0		
Fuselage	43 906	1920.0	103.0
Landing gear	32 326	1850.4	70.0
Nacelle	19 790	2330.0	13.0
Structure total	153 381	2016.9	79.2
Engines	50 665	2435.0	13.0
Thrust reverser	0		
Miscellaneous systems	2 341	1481.5	45.7
Fuel system	8 026	2083.9	89.5
Propulsion total	61 031	2352.2	24.3
Surface controls	7 399	2193.6	122.2
Auxiliary power unit	1 578	2600.0	50.0
Instruments	2 141	1172.4	103.0
Hydraulics	5 449	1958.6	103.0
Electrical	3 888	1293.5	103.0
Avionics	1 449	860.0	136.0
Furnishings and equipment	20 388	1842.0	
Air conditioning	6 741	1890.0	103.0
Anti-icing	215	1948.0	65.4
System and equipment total	49 246	1837.7	61.2
Weight empty	263 658	2061.1	63.1
Flight crew and baggage (2)	450	528.0	144.0
Cabin crew and baggage (7)	1 130	1842.0	98.0
Unusuable fuel	3 269	2083.9	89.5
Engine oil	914	2435.0	13.0
Passenger service	3 560	1842.0	98.0
Cargo containers	0		
Operating weight	272 981	2056.3	64.0
Passengers (250)	41 250	1842.0	98.0
Passenger baggage	11 000	1300.0	75.0
Miscellaneous items	2 565	1920.0	103.0
Cargo	0		
Zero-fuel weight	327 796	2002.9	69.0
Mission fuel	385 900	1849.0	106.1
Gross weight	713 696	1919.7	89.0

Table III. Numerical Model for Zero-Lift Drag Analysis

```
 2AST31 WAVE DRAG MODEL
  1  1 -1  1  1  0  0 11 20  1 19 20                         5 10  1 10
12185. 129.70 160.0                                                          SCXCG
0.0    .50    .75    1.25   2.50   5.00   7.50   10.0   15.0   20.0         XAF1
25.0   30.0   35.0   40.0   50.0   60.0   70.0   80.0   90.0   100.0        XAF2
16.358 7.5    -2.60  192.789                                                 WORG   3
25.333 9.333  -3.57  183.814                                                 WORG   4
56.096 15.00  -4.80  153.052                                                 WORG   5
83.238 20.00  -6.69  125.909                                                 WORG   6
121.23827.00  -8.28  91.110                                                  WORG   7
160.33334.202 -9.00  55.309                                                  WORG   8
171.33340.00  -8.00  47.281                                                  WORG   9
188.66753.00  -6.47  36.725                                                  WORG  10
210.49568.00  -5.60  25.150                                                  WORG  11
219.63872.00  -5.90  21.320                                                  WORG  12
238.40 75.30  -6.00  8.400                                                   WORG  13
  0.000  0.027  0.037  0.052  0.052 -0.150 -0.147 -0.767 -1.575 -2.392       ZORD 3-1
 -3.158 -3.908 -4.625 -5.275 -6.292 -7.133 -7.775 -8.258 -8.533 -8.751       ZORD 3-2
  0.000  0.031  0.048  0.075  0.160  0.217  0.037 -0.202 -0.798 -1.487       ZORD 4-1
 -2.209 -2.917 -3.534 -4.132 -5.163 -5.968 -6.603 -7.082 -7.436 -7.739       ZORD 4-2
  0.000  0.064  0.096  0.155  0.286  0.484  0.545  0.504  0.300 -0.049       ZORD 5-1
 -0.467 -0.943 -1.442 -1.959 -2.983 -3.946 -4.803 -5.525 -6.087 -6.460       ZORD 5-2
  0.000  0.065  0.097  0.157  0.295  0.510  0.638  0.700  0.690  0.570       ZORD 6-1
  0.358  0.105 -0.206 -0.540 -1.260 -2.001 -2.722 -3.395 -3.990 -4.475       ZORD 6-2
  0.000  0.053  0.078  0.128  0.247  0.452  0.614  0.725  0.841  0.880       ZORD 7-1
  0.887  0.831  0.730  0.606  0.292 -0.094 -0.507 -0.923 -1.326 -1.697       ZORD 7-2
  0.000  0.023  0.034  0.056  0.112  0.218  0.320  0.418  0.550  0.614       ZORD 8-1
  0.649  0.682  0.704  0.726  0.764  0.786  0.806  0.824  0.827  0.830       ZORD 8-2
  0.000  0.002  0.003  0.005  0.011  0.021  0.030  0.039  0.054  0.066       ZORD 9-1
  0.077  0.089  0.103  0.114  0.134  0.144  0.150  0.149  0.151  0.140       ZORD 9-2
  0.000 -0.006 -0.009 -0.015 -0.029 -0.057 -0.084 -0.111 -0.162 -0.209       ZORD10-1
 -0.253 -0.295 -0.335 -0.372 -0.437 -0.487 -0.521 -0.537 -0.544 -0.548       ZORD10-2
  0.000 -0.002 -0.003 -0.004 -0.008 -0.017 -0.025 -0.032 -0.048 -0.063       ZORD11-1
 -0.078 -0.093 -0.107 -0.120 -0.147 -0.168 -0.181 -0.188 -0.190 -0.187       ZORD11-2
  0.000  0.000  0.000  0.000  0.000  0.000  0.000  0.000 -0.001 -0.002       ZORD12-1
 -0.004 -0.006 -0.008 -0.011 -0.020 -0.027 -0.036 -0.043 -0.044 -0.040       ZORD12-2
  0.000  0.000  0.000  0.000  0.001  0.002  0.002  0.003  0.005  0.006       ZORD13-1
  0.008  0.009  0.011  0.013  0.016  0.019  0.022  0.025  0.028  0.031       ZORD13-2
0.0    .061   .108   .182   .287   .405   .488   .562   .685   .793         WORD 3-1
.886   .953   .990   .996   .994   .962   .838   .586   .283   0.0          WORD 3-2
0.0    .1333  .1599  .2037  .2970  .4151  .5017  .5741  .6893  .7788        WORD 4-1
.8473  .8987  .9330  .9511  .9330  .8340  .6731  .4656  .2352  0.0          WORD 4-2
0.0    .1424  .1709  .2177  .3174  .4435  .5631  .6134  .7365  .8322        WORD 5-1
.9054  .9603  .9970  1.0163 .9970  .8912  .7192  .4975  .2513  0.0          WORD 5-2
0.0    .1573  .1887  .2404  .3505  .4898  .5921  .6774  .8134  .9190        WORD 6-1
.9999  1.0605 1.1010 1.1223 1.1010 .9841  .7943  .5494  .2775  0.0          WORD 6-2
0.0    .2013  .2428  .3087  .4324  .5952  .7159  .8197  .9849  1.1113       WORD 7-1
1.2088 1.2801 1.3280 1.3523 1.3244 1.1826 .9533  .6581  .3331  0.0          WORD 7-2
```

Table III. Concluded

0.0	.0515	.0769	.1289	.2527	.4939	.7314	.9557	1.3482	1.5946	WORD 8-1
1.7332	1.8341	1.9019	1.9358	1.8942	1.6896	1.3591	.9374	.4750	0.0	WORD 8-2
0.0	.0532	.0793	.1330	.2607	.5095	.7545	.9859	1.3908	1.6450	WORD 9-1
1.7880	1.8920	1.9620	1.9970	1.9540	1.7430	1.4020	.9672	.4900	0.0	WORD 9-2
0.0	.0507	.0757	.1269	.2486	.4859	.7196	.9402	1.3264	1.5688	WORD10-1
1.7052	1.8044	1.8712	1.9045	1.8635	1.6623	1.3371	.9222	.4673	0.0	WORD10-2
0.0	.0465	.0694	.1174	.2281	.4458	.6602	.8627	1.2169	1.4394	WORD11-1
1.5645	1.6555	1.7168	1.7474	1.7098	1.5251	1.2268	.8461	.4288	0.0	WORD11-2
0.0	.0528	.0789	.1323	.2576	.4997	.7411	.9698	1.3685	1.6196	WORD12-1
1.7589	1.8600	1.9272	1.9616	1.9110	1.6956	1.3556	.9312	.4710	0.0	WORD12-2
0.0	.0528	.0789	.1323	.2576	.4997	.7411	.9698	1.3685	1.6196	WORD13-1
1.7589	1.8600	1.9272	1.9616	1.9110	1.6956	1.3556	.9312	.4710	0.0	WORD13-2
0.0	10.0	20.0	40.0	60.0	80.0	100.0	120.0	140.0	160.0	XFUS 1
170.0	180.0	190.0	200.0	218.47	230.0	245.0	260.0	280.0	298.0	XFUS 2
0.0	-1.01	-1.83	-3.43	-4.72	-5.86	-6.76	-7.36	-7.85	-8.27	ZFUS 1
-8.48	-8.68	-8.88	-8.87	-8.44	-7.90	-6.89	-5.58	-3.43	-1.17	ZFUS 2
0.0	13.5	28.0	57.0	80.5	97.0	112.0	128.0	141.5	144.7	AFUS 1
144.9	143.5	141.4	137.5	118.5	101.7	72.3	45.7	16.7	0.0	AFUS 2
180.0	9.7	-14.70								PODORG 1
0.0	5.0	10.0	15.0	20.0	25.0	27.5	30.0	35.0	38.47	XPOD 1
3.195	3.387	3.536	3.678	3.810	3.937	3.989	3.981	3.893	3.804	PODR 1
180.0	16.7	-14.27								PODORG 2
0.0	5.0	10.0	15.0	20.0	25.0	27.5	30.0	35.0	38.47	XPOD 2
3.195	3.387	3.536	3.678	3.810	3.937	3.989	3.981	3.893	3.804	PODR 2
180.0	23.7	-13.29								POGORG 3
0.0	5.0	10.0	15.0	20.0	25.0	27.5	30.0	35.0	38.47	XPOD 3
3.195	3.387	3.536	3.678	3.810	3.937	3.989	3.981	3.893	3.804	PODR 3
171.75	11.4	-12.00								PODORG 4
0.0	3.25	5.75	8.25	10.75	13.25	15.75	18.25	23.25	28.25	XPOD 4
0.0	.626	.937	1.128	1.223	1.194	1.095	.982	.67	0.0	PODR 4
171.75	21.8	-11.0								PODORG 5
0.0	3.25	5.75	8.25	10.75	13.25	15.75	18.25	23.25	28.25	XPOD 5
0.0	.626	.937	1.128	1.223	1.194	1.095	.982	.67	0.0	PODR 5
270.5	0.0	-1.00	27.5	292.6	0.0	7.0	5.4			FNORG
0.0	10.0	20.0	30.0	40.0	50.0	60.0	70.0	80.0	100.0	XFIN
0.0	.45	.80	1.05	1.20	1.25	1.20	1.05	.80	0.0	FNORD

Table IV. Numerical Model for Analysis at Lift

```
      2AST3I   FUSELAGE AS WING ANLZ/SUBAERF MODEL INCLUDING PODS
 1  1  0  1   0  0  2 14 20                                5 10
12185.  129.70 160.0                                                       SCXCG
0.0     .50     .75     1.25    2.50    5.00    7.50    10.0    15.0    20.0     XAF1
25.0    30.0    35.0    40.0    50.0    60.0    70.0    80.0    90.0    100.0    XAF2
0.0     0.0     0.0     209.147                                                  WORG   1
1.163   2.0     -.70    207.984                                                  WORG  1A
7.270   5.0     -1.70   201.877                                                  WORG   2
16.358 7.5      -2.60   192.789                                                  WORG   3
25.333 9.333    -3.57   183.814                                                  WORG   4
56.096 15.00    -4.80   153.052                                                  WORG   5
83.238 20.00    -6.69   125.909                                                  WORG   6
121.23827.00    -8.28   91.110                                                   WORG   7
160.33334.202 -9.00     55.309                                                   WORG   8
171.33340.00    -8.00   47.281                                                   WORG   9
188.66753.00    -6.47   36.725                                                   WORG  10
210.49568.00    -5.60   25.150                                                   WORG  11
219.63872.00    -5.90   21.320                                                   WORG  12
238.40 75.30    -6.00   8.400                                                    WORG  13
  0.000 -0.069 -0.102 -0.176 -0.368 -0.811 -1.261 -1.698 -2.478 -3.117   ZORD 1-1
 -3.700 -4.250 -4.750 -5.196 -5.933 -6.583 -7.160 -7.704 -8.219 -8.716   ZORD 1-2
  0.000 -0.069 -0.102 -0.176 -0.368 -0.811 -1.262 -1.718 -2.560 -3.288   ZORD1A-1
 -3.927 -4.480 -4.939 -5.366 -6.075 -6.680 -7.226 -7.741 -8.230 -8.731   ZORD1A-2
  0.000 -0.028 -0.044 -0.079 -0.190 -0.480 -0.832 -1.211 -2.059 -2.895   ZORD 2-1
 -3.685 -4.420 -5.009 -5.487 -6.241 -6.800 -7.254 -7.671 -8.079 -8.465   ZORD 2-2
  0.000  0.027  0.037  0.052  0.052 -0.150 -0.147 -0.767 -1.575 -2.392   ZORD 3-1
 -3.158 -3.908 -4.625 -5.275 -6.292 -7.133 -7.775 -8.258 -8.533 -8.751   ZORD 3-2
  0.000  0.031  0.048  0.075  0.160  0.217  0.037 -0.202 -0.798 -1.487   ZORD 4-1
 -2.209 -2.917 -3.534 -4.132 -5.163 -5.968 -6.603 -7.082 -7.436 -7.739   ZORD 4-2
  0.000  0.064  0.096  0.155  0.286  0.484  0.545  0.504  0.300 -0.049   ZORD 5-1
 -0.467 -0.943 -1.442 -1.959 -2.983 -3.946 -4.803 -5.525 -6.087 -6.460   ZORD 5-2
  0.000  0.065  0.097  0.157  0.295  0.510  0.638  0.700  0.690  0.570   ZORD 6-1
  0.358  0.105 -0.206 -0.540 -1.260 -2.001 -2.722 -3.395 -3.990 -4.475   ZORD 6-2
  0.000  0.053  0.078  0.128  0.247  0.452  0.614  0.725  0.841  0.880   ZORD 7-1
  0.887  0.831  0.730  0.606  0.292 -0.094 -0.507 -0.923 -1.326 -1.697   ZORD 7-2
  0.000  0.023  0.034  0.056  0.112  0.218  0.320  0.418  0.550  0.614   ZORD 8-1
  0.649  0.682  0.704  0.726  0.764  0.786  0.806  0.824  0.827  0.830   ZORD 8-2
  0.000  0.002  0.003  0.005  0.011  0.021  0.030  0.039  0.054  0.066   ZORD 9-1
  0.077  0.089  0.103  0.114  0.134  0.144  0.150  0.149  0.151  0.140   ZORD 9-2
  0.000 -0.006 -0.009 -0.015 -0.029 -0.057 -0.084 -0.111 -0.162 -0.209   ZORD10-1
 -0.253 -0.295 -0.335 -0.372 -0.437 -0.487 -0.521 -0.537 -0.544 -0.548   ZORD10-2
  0.000 -0.002 -0.003 -0.004 -0.008 -0.017 -0.025 -0.032 -0.048 -0.063   ZORD11-1
 -0.078 -0.093 -0.107 -0.120 -0.147 -0.168 -0.181 -0.188 -0.190 -0.187   ZORD11-2
  0.000  0.000  0.000  0.000  0.000  0.000  0.000  0.000 -0.001 -0.002   ZORD12-1
 -0.004 -0.006 -0.008 -0.011 -0.020 -0.027 -0.036 -0.043 -0.044 -0.040   ZORD12-2
  0.000  0.000  0.000  0.000  0.001  0.002  0.002  0.003  0.005  0.006   ZORD13-1
  0.008  0.009  0.011  0.013  0.016  0.019  0.022  0.025  0.028  0.031   ZORD13-2
```

Table IV. Concluded

0.0	.10	.14	.23	.44	.79	1.07	1.30	1.72	2.05	WORD 1-1
2.25	2.41	2.56	2.68	2.83	2.97	3.43	3.70	3.55	2.69	WORD 1-2
0.0	.08	.14	.20	.37	.62	.78	.92	1.34	1.70	WORD 1A1
1.96	2.17	2.33	2.49	2.68	2.83	3.17	3.29	2.92	2.33	WORD 1A2
0.0	.08	.12	.21	.30	.41	.50	.59	.70	.86	WORD 2-1
1.08	1.31	1.58	1.93	2.33	2.29	1.97	1.68	1.41	1.04	WORD 2-2
0.0	.061	.108	.182	.287	.405	.488	.562	.685	.793	WORD 3-1
.886	.953	.990	.996	.994	.962	.838	.586	.283	0.0	WORD 3-2
0.0	.1333	.1599	.2037	.2970	.4151	.5017	.5741	.6893	.7788	WORD 4-1
.8473	.8987	.9330	.9511	.9330	.8340	.6731	.4656	.2352	0.0	WORD 4-2
0.0	.1424	.1709	.2177	.3174	.4435	.5631	.6134	.7365	.8322	WORD 5-1
.9054	.9603	.9970	1.0163	.9970	.8912	.7192	.4975	.2513	0.0	WORD 5-2
0.0	.1573	.1887	.2404	.3505	.4898	.5921	.6774	.8134	.9190	WORD 6-1
.9999	1.0605	1.1010	1.1223	1.1010	.9841	.7943	.5494	.2775	0.0	WORD 6-2
0.0	.2013	.2428	.3087	.4324	.5952	.7159	.8197	.9849	1.1113	WORD 7-1
1.2088	1.2801	1.3280	1.3523	1.3244	1.1826	.9533	.6581	.3331	0.0	WORD 7-2
0.0	.0515	.0769	.1289	.2527	.4939	.7314	.9557	1.3482	1.5946	WORD 8-1
1.7332	1.8341	1.9019	1.9358	1.8942	1.6896	1.3591	.9374	.4750	0.0	WORD 8-2
0.0	.0532	.0793	.1330	.2607	.5095	.7545	.9859	1.3908	1.6450	WORD 9-1
1.7880	1.8920	1.9620	1.9970	1.9540	1.7430	1.4020	.9672	.4900	0.0	WORD 9-2
0.0	.0507	.0757	.1269	.2486	.4859	.7196	.9402	1.3264	1.5688	WORD10-1
1.7052	1.8044	1.8712	1.9045	1.8635	1.6623	1.3371	.9222	.4673	0.0	WORD10-2
0.0	.0465	.0694	.1174	.2281	.4458	.6602	.8627	1.2169	1.4394	WORD11-1
1.5645	1.6555	1.7168	1.7474	1.7098	1.5251	1.2268	.8461	.4288	0.0	WORD11-2
0.0	.0528	.0789	.1323	.2576	.4997	.7411	.9698	1.3685	1.6196	WORD12-1
1.7589	1.8600	1.9272	1.9616	1.9110	1.6956	1.3556	.9312	.4710	0.0	WORD12-2
0.0	.0528	.0789	.1323	.2576	.4997	.7411	.9698	1.3685	1.6196	WORD13-1
1.7589	1.8600	1.9272	1.9616	1.9110	1.6956	1.3556	.9312	.4710	0.0	WORD13-2
180.0	9.7	-14.70								PODORG 1
0.0	5.0	10.0	15.0	20.0	25.0	27.5	30.0	35.0	38.47	XPOD 1
3.195	3.387	3.536	3.678	3.810	3.937	3.989	3.981	3.893	3.804	PODR 1
180.0	16.7	-14.27								PODORG 2
0.0	5.0	10.0	15.0	20.0	25.0	27.5	30.0	35.0	38.47	XPOD 2
3.195	3.387	3.536	3.678	3.810	3.937	3.989	3.981	3.893	3.804	PODR 2
180.0	23.7	-13.29								POGORG 3
0.0	5.0	10.0	15.0	20.0	25.0	27.5	30.0	35.0	38.47	XPOD 3
3.195	3.387	3.536	3.678	3.810	3.937	3.989	3.981	3.893	3.804	PODR 3
171.75	11.4	-12.00								PODORG 4
0.0	3.25	5.75	8.25	10.75	13.25	15.75	18.25	23.25	28.25	XPOD 4
0.0	.626	.937	1.128	1.223	1.194	1.095	.982	.67	0.0	PODR 4
171.75	21.8	-11.0								PODORG 5
0.0	3.25	5.75	8.25	10.75	13.25	15.75	18.25	23.25	28.25	XPOD 5
0.0	.626	.937	1.128	1.223	1.194	1.095	.982	.67	0.0	PODR 5

Table V. GE 2114 Q (Modified GE 21/J11-B14a) Engine Performance

MACH NUMBER	ALTITUDE	NET THRUST	FUEL FLOW
3.0000	65000.0	20121.0	29563.0
3.0000	65000.0	12824.0	16467.0
3.0000	60000.0	25898.3	38083.0
3.0000	60000.0	16396.3	20970.0
3.0000	60000.0	13955.3	17947.0
3.0000	60000.0	11490.3	15069.0
3.0000	60000.0	8542.3	11895.0
3.0000	60000.0	6200.0	8891.0
3.0000	60000.0	3100.0	5872.0
3.0000	60000.0	0.0	1660.0
3.0000	58700.0	27631.8	40635.0
3.0000	58700.0	17472.8	22328.0
3.0000	55000.0	33116.4	48683.0
3.0000	55000.0	20911.4	26673.0
2.5200	55000.0	27242.9	38240.0
2.5200	55000.0	19680.9	24100.0
2.5200	51500.0	32381.7	45467.0
2.5200	51500.0	23336.7	28529.0
2.5200	45000.0	44436.6	62374.0
2.5200	45000.0	31969.6	38999.0
2.2900	55000.0	23628.1	32580.0
2.2900	55000.0	17642.1	21225.0
2.2900	48100.0	32906.6	45270.0
2.2900	48100.0	24531.6	29398.0
2.2900	45000.0	38194.1	52503.0
2.2900	45000.0	28468.1	34079.0
1.8300	45000.0	27731.6	36405.0
1.8300	45000.0	22096.6	25520.0
1.8300	41300.0	33141.7	43447.0
1.8300	41300.0	26388.7	30432.0
1.8300	35000.0	44602.8	58539.0
1.8300	35000.0	35665.8	41300.0
1.3700	40000.0	21549.4	30112.0
1.3700	40000.0	15826.4	18259.0

Table V. Continued

1.3700	40000.0	21549.4	30112.0
1.3700	40000.0	15826.4	18259.0
1.3700	30000.0	33877.2	47567.0
1.3700	30000.0	25479.2	30214.0
1.1500	35000.0	22300.8	30923.0
1.1500	35000.0	16398.8	17716.0
1.1500	31000.0	26567.7	36945.0
1.1500	31000.0	19809.7	21815.0
1.0900	45000.0	13630.1	18256.0
1.0900	45000.0	10307.1	10342.0
1.0900	35000.0	21980.3	29397.0
1.0900	35000.0	16597.3	16588.0
1.0900	35000.0	14930.3	14663.0
1.0900	35000.0	12725.3	12408.0
1.0900	35000.0	10019.6	10018.0
1.0900	35000.0	8197.1	8492.0
1.0900	35000.0	6279.6	6961.0
1.0900	35000.0	0.0	1541.0
1.0900	30000.0	27369.8	36688.0
1.0900	30000.0	20987.8	21490.0
1.0900	25000.0	33745.2	45333.0
1.0900	25000.0	26285.2	27568.0
1.0300	45000.0	12952.5	17297.0
1.0300	45000.0	9802.5	9643.0
1.0300	35000.0	20889.6	27851.0
1.0300	35000.0	15777.6	15449.0
1.0300	35000.0	14203.6	13648.0
1.0300	35000.0	12127.6	11550.0
1.0300	35000.0	9676.6	9411.0
1.0300	35000.0	7944.2	7980.0
1.0300	35000.0	6125.9	6576.0
1.0300	35000.0	0.0	1456.0
1.0300	25000.0	32106.1	42970.0
1.0300	25000.0	24979.1	25654.0
.9700	35000.0	19967.9	26592.0
.9700	35000.0	15101.9	14572.0
.9700	30000.0	24887.7	33203.0
.9700	30000.0	19089.7	18864.0

Table V. Concluded

.9700	30000.0	24887.7	33203.0
.9700	30000.0	19089.7	18864.0
.9700	25000.0	30715.6	41046.0
.9700	25000.0	23899.6	24185.0
.8000	35000.0	17400.0	23142.0
.8000	35000.0	13400.0	12797.0
.8000	25000.0	27400.0	36442.0
.8000	25000.0	21250.0	21250.0
.8000	15000.0	41111.8	54443.0
.8000	15000.0	33052.8	33451.0
.5700	10000.0	44809.0	55170.0
.5700	10000.0	27590.4	30407.0
.5700	10000.0	24891.4	27477.0
.5700	10000.0	20237.0	22948.0
.5700	10000.0	16002.1	19258.0
.5700	10000.0	12972.4	16730.0
.5700	10000.0	9557.3	13547.0
.5700	10000.0	0.0	4032.0
.5700	1500.0	60620.5	75271.0
.5700	1500.0	37316.1	41779.0
.3400	10000.0	42777.2	48782.0
.3400	10000.0	27487.2	27543.0
.3400	1500.0	57495.9	70001.0
.3400	1500.0	36529.9	38126.0
.3400	1500.0	33118.9	34346.0
.3400	1500.0	27680.9	29253.0
.3400	1500.0	22331.9	24539.0
.3400	1500.0	18581.9	21382.0
.3400	1500.0	14570.5	17734.0
.3400	1500.0	0.0	5555.0
.3400	0.0	60311.8	73595.0
.3400	0.0	38362.8	40319.0
0.0000	1500.0	58218.0	63289.0
0.0000	1500.0	39262.0	34613.0
0.0000	0.0	61271.0	67418.0
0.0000	0.0	41245.0	36588.0
0.0000	0.0	37816.0	32993.0
0.0000	0.0	32170.0	27961.0
0.0000	0.0	26831.0	23567.0
0.0000	0.0	23190.0	20741.0
0.0000	0.0	19616.0	17758.0
0.0000	0.0	0.0	5546 0

Table VI. Mission Summary

[SREF = 12 185 ft^2, OWE = 272 978 lb, Payload = 54 815 lb, Maximum fuel = 385 903 lb]

		Fuel, lb		Time, min		Distance, n.mi.		Mach number		Altitude, ft	
Segment	Initial weight, lb	Segment	Total	Segment	Total	Segment	Total	Start	End	Start	End
Taxi out	713 696	3 697	3 697	10.0	10.0						
Takeoff	709 999	2 542	6 239	0.7	10.7				0.300		0
Climb	707 457	52 773	59 012	11.5	22.2	186.1	186.1	0.300	3.000	0	65 671
Cruise	654 685	264 534	323 545	203.7	225.9	5 959.4	6 145.4	3.000	3.000	65 671	70 000
Descent	390 151	9 772	333 318	35.3	261.1	354.6	6 500.0	3.000	0.300	70 000	0
Reserves	380 378	52 585	385 903								
Zero fuel	327 793										

Design range, n.mi.	**6500.0**
Flight time, min	**250.4**
Block time, hr	**4.44**
Block fuel, lb	**335 166**
ATA traffic allowance, n.mi.	**323.1**
Air maneuver, n.mi.	**175.7**
Airport traffic allowance, n.mi.	**17.4**
Airway distance factor, n.mi.	**130.0**
ATA range, n.mi.	**6500.0**

Table VII. Reserve Details

Segment	Fuel weight, lb
Missed approach (0.23 min at maximum afterburner)	842
Climb	11 315
Cruise ($M = 0.92$, $h = 45\,000$ ft)	3 657
Hold ($M = 0.90$, $h = 45\,000$ ft)	12 401
Descent	8 002
Subtotal	36 217
5% trip ($0.05 \times 327\,079$)	16 354
Total	$52\,571 \approx 52\,585$
Used in mission	52 585

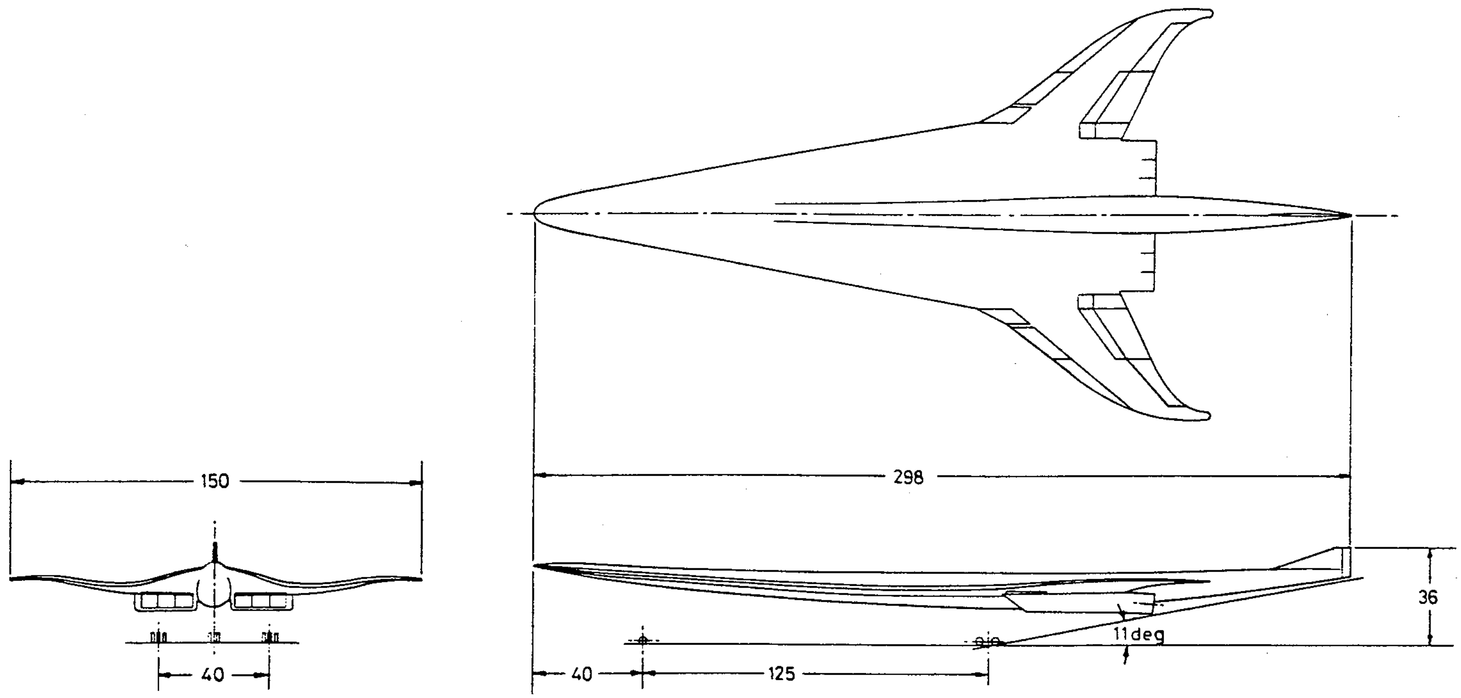

Figure 1. General arrangement. Linear dimensions are in feet.

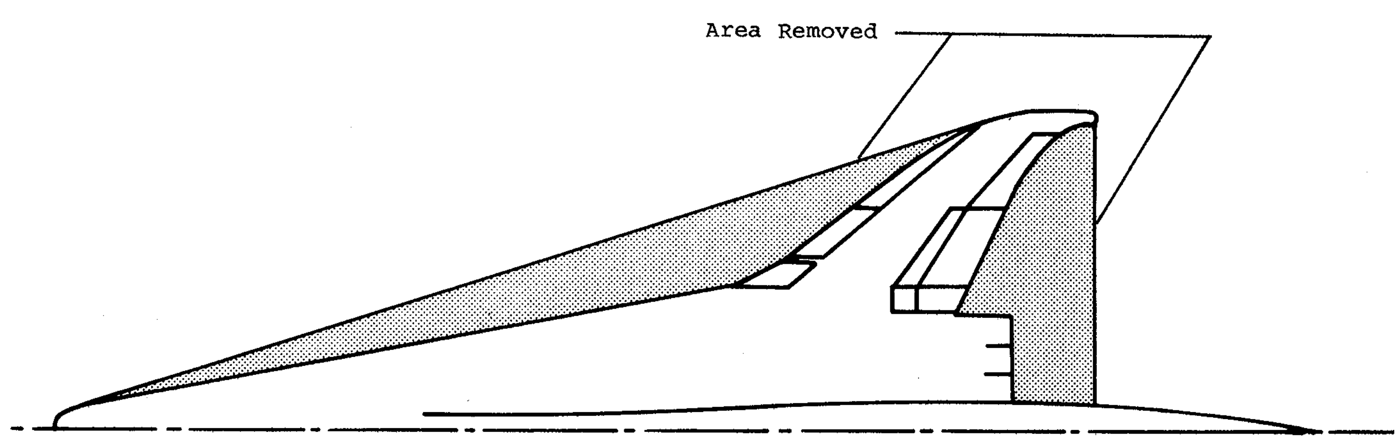

Figure 2. Modifications to delta planform.

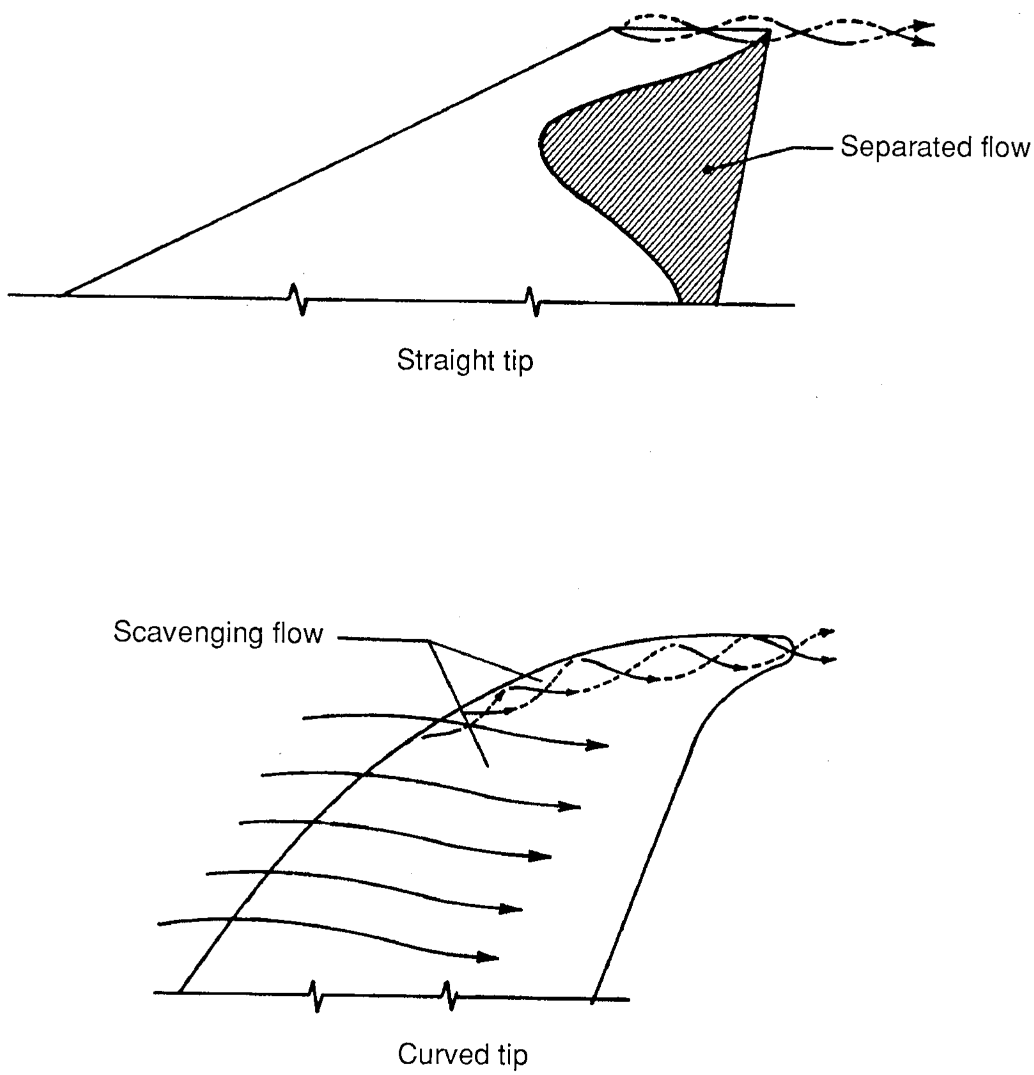

Figure 3. Tip flow for straight tip and curved tip.

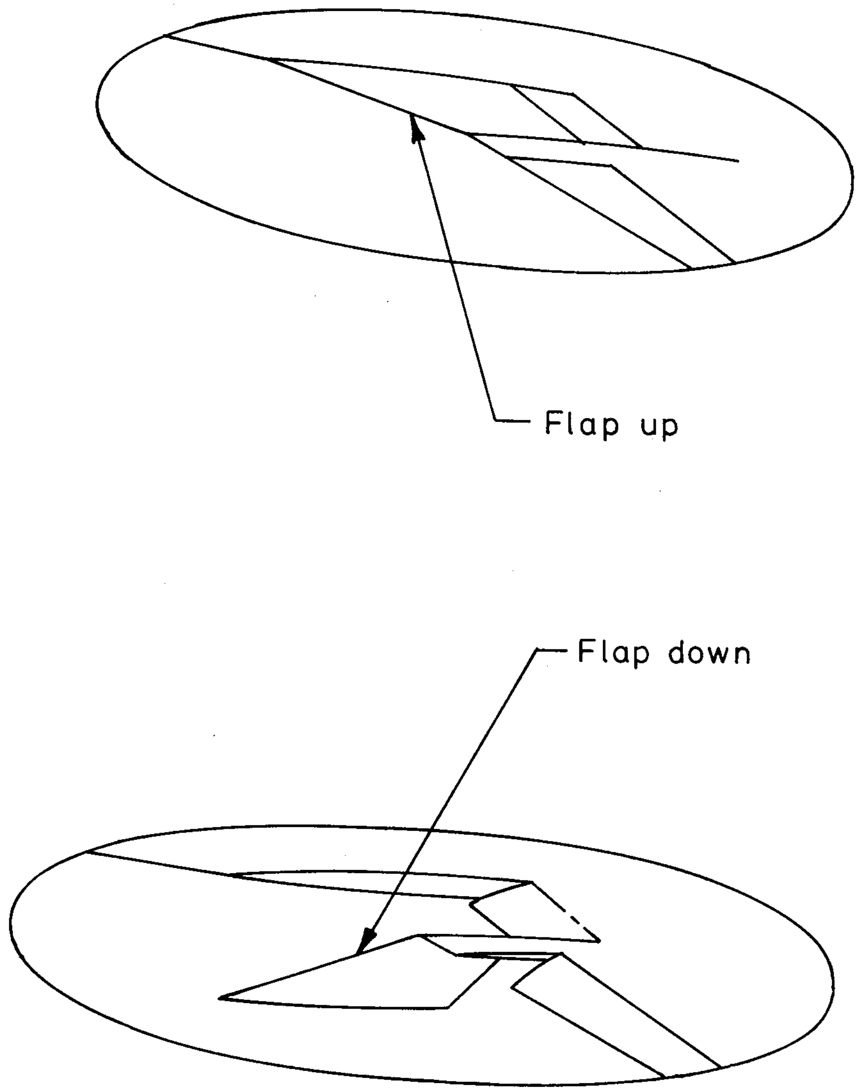

Figure 4. Notch flap.

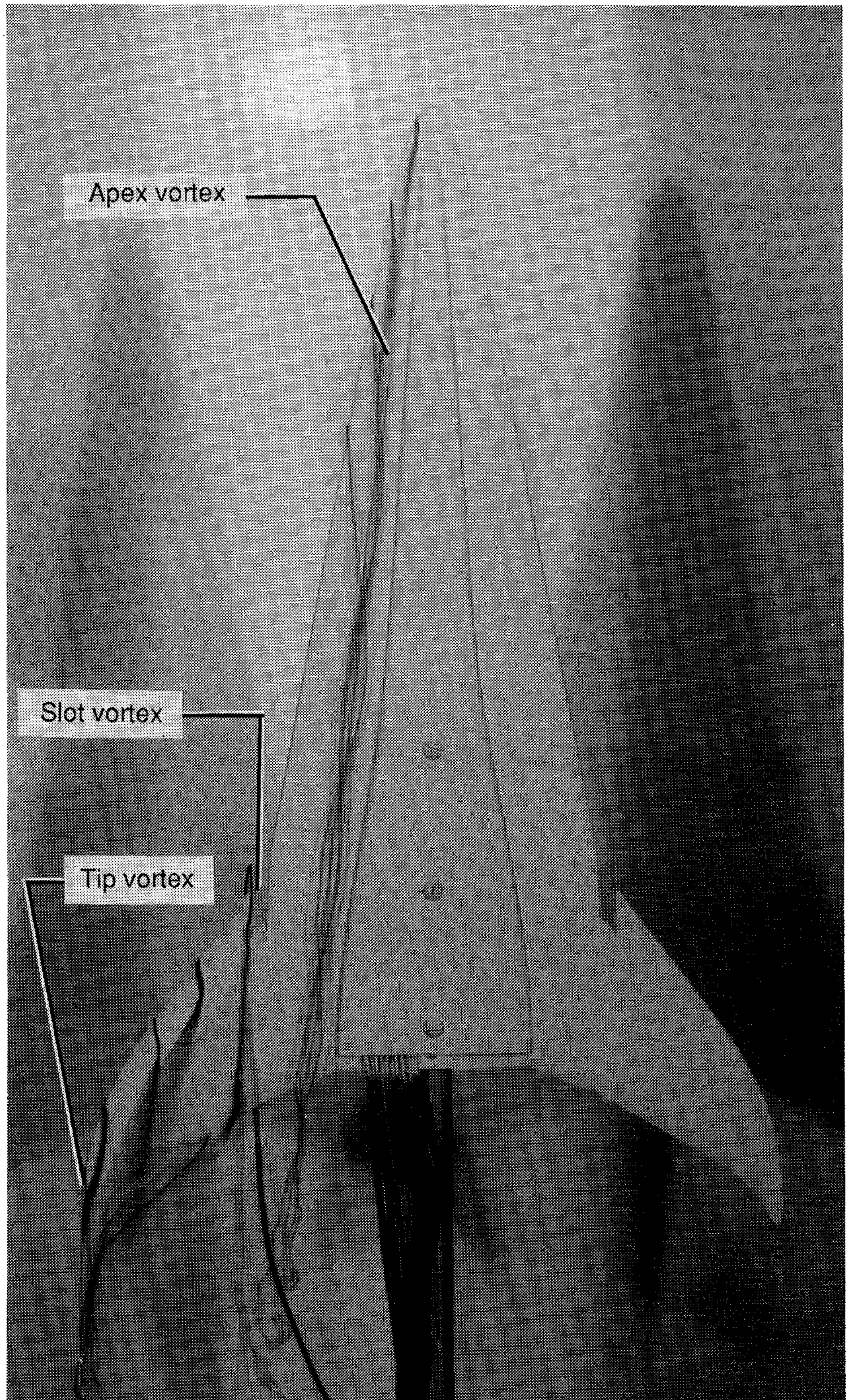

L-88-104

Figure 5. Water tunnel model at $\alpha = 5^{\circ}$.

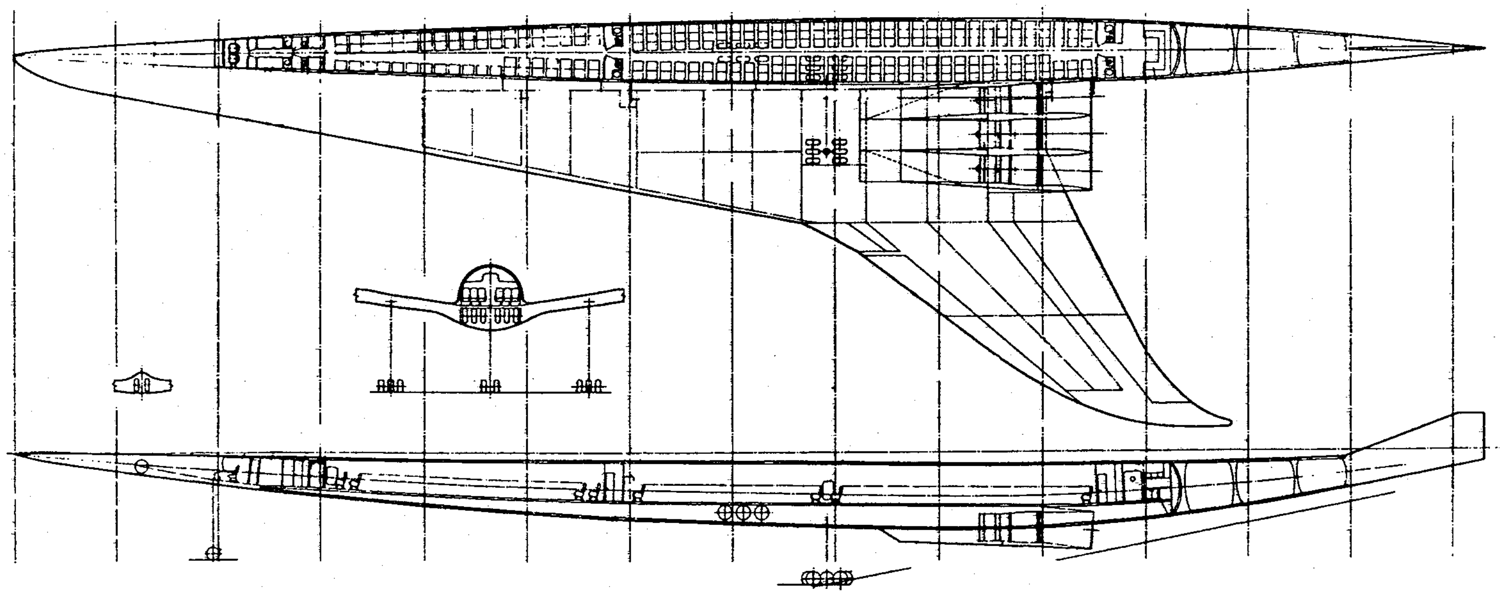

Figure 6. Interior arrangement.

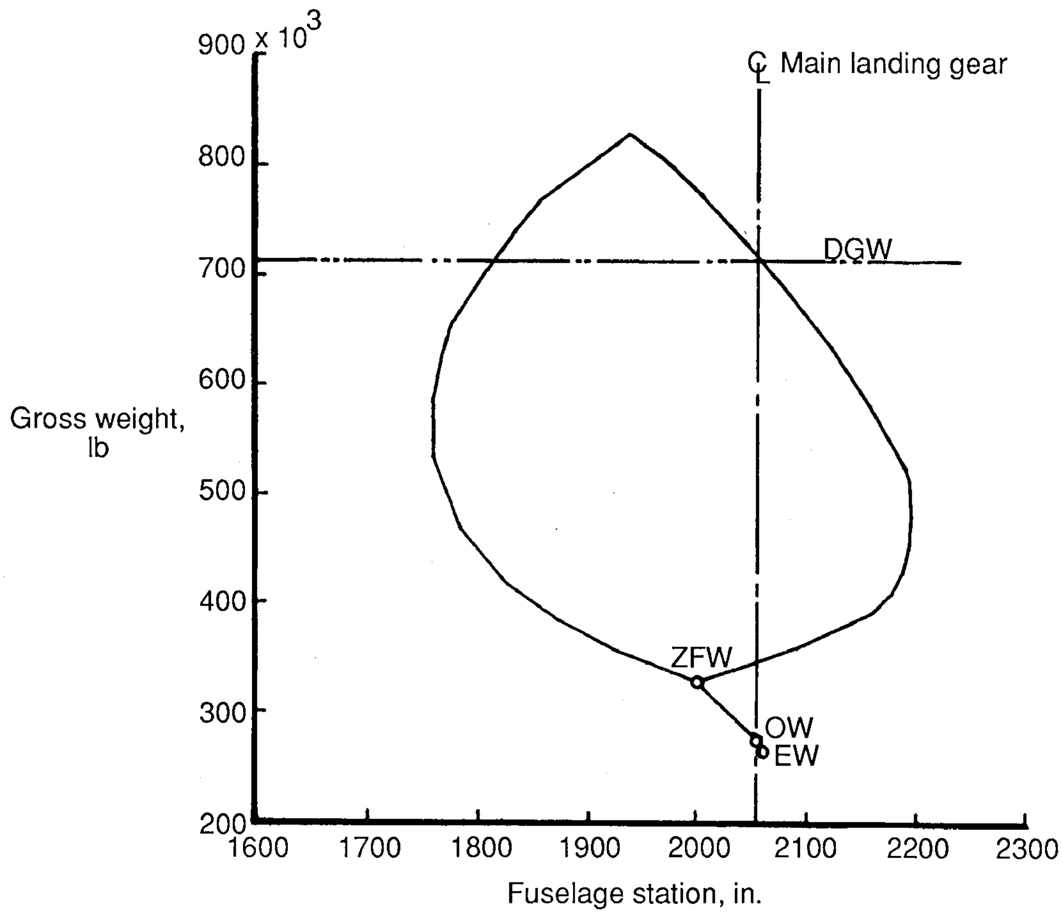

Figure 7. Center-of-gravity diagram.

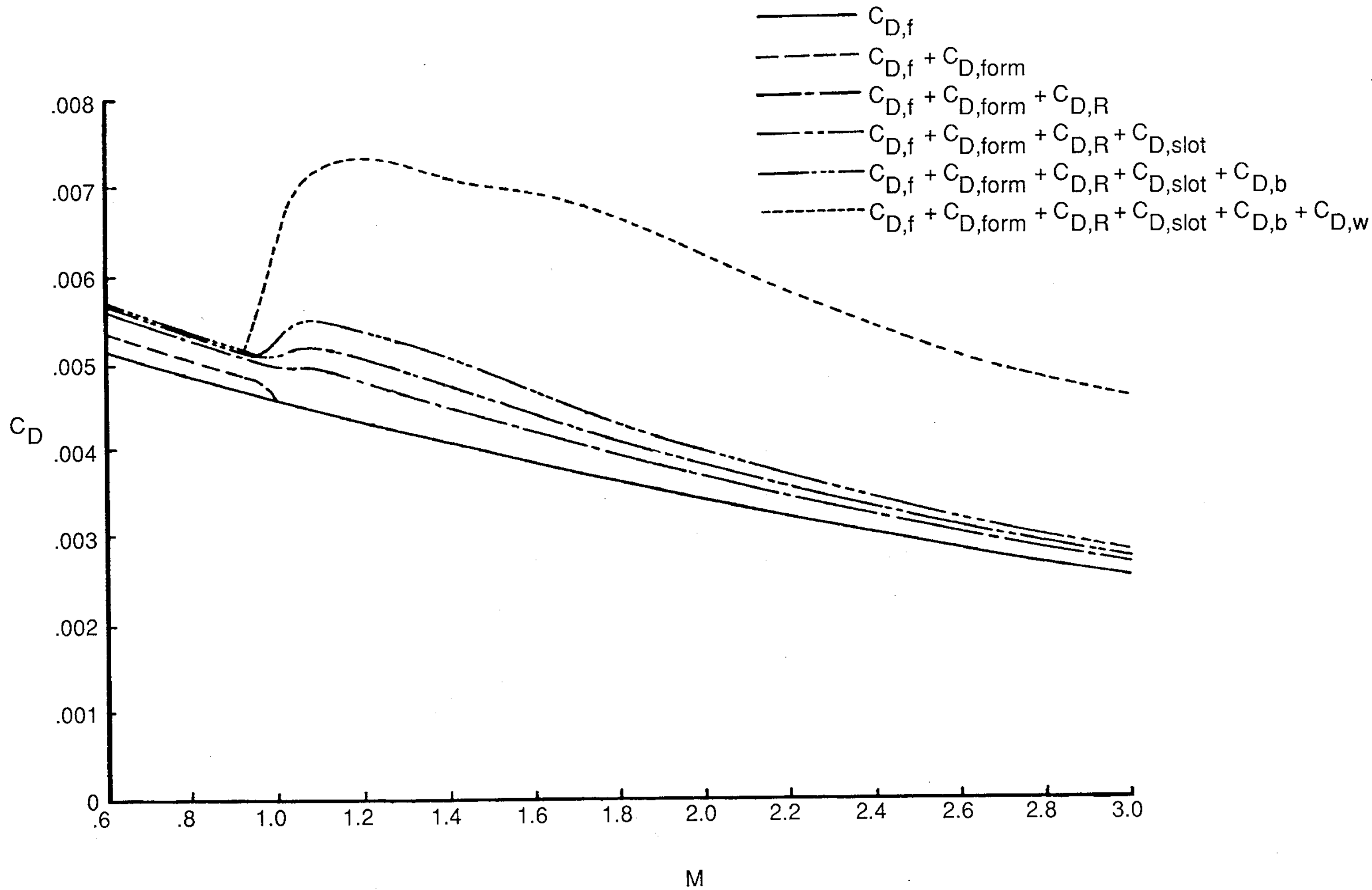

Figure 8. Buildup of zero-lift drag coefficient, $h = 40\,000$ ft.

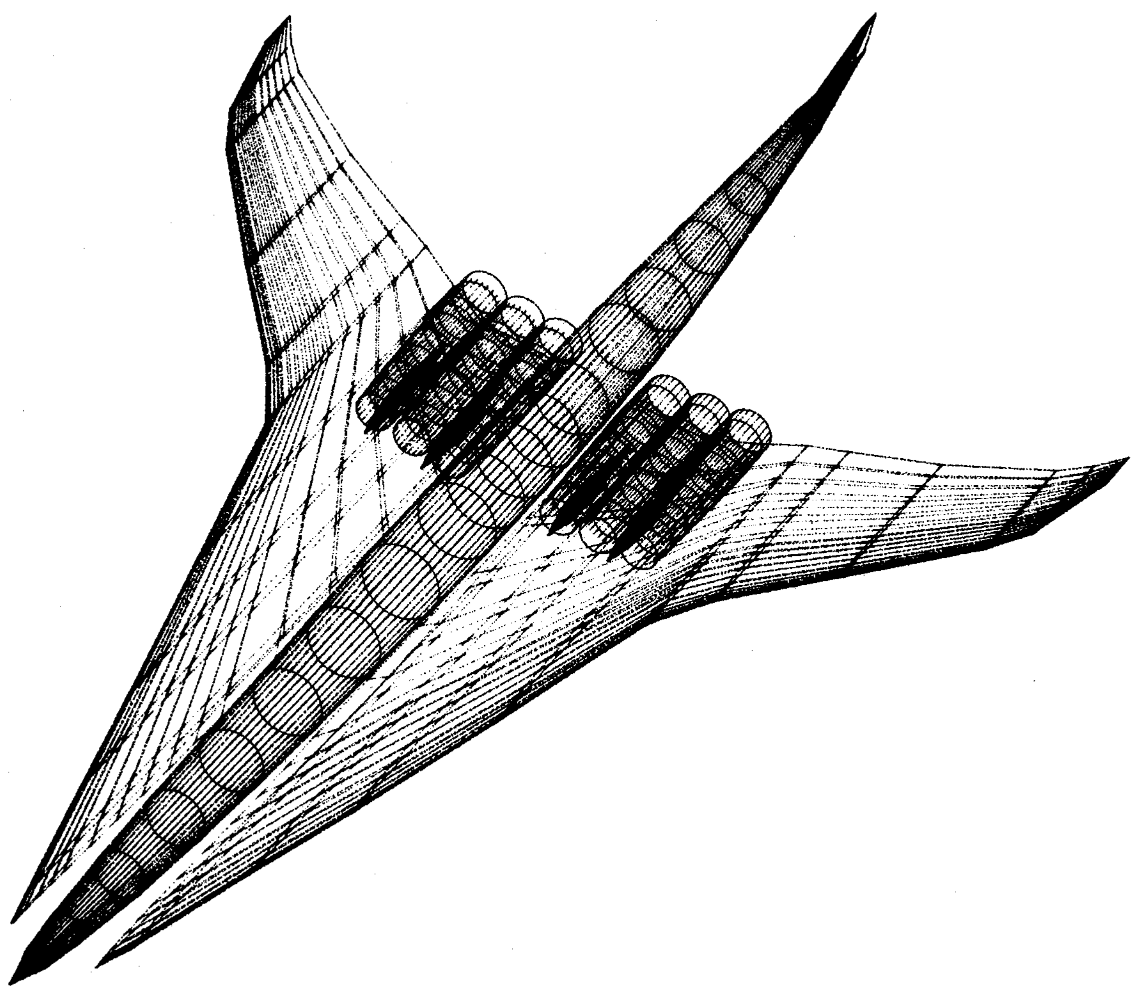

Figure 9. Numerical model for wave-drag analysis.

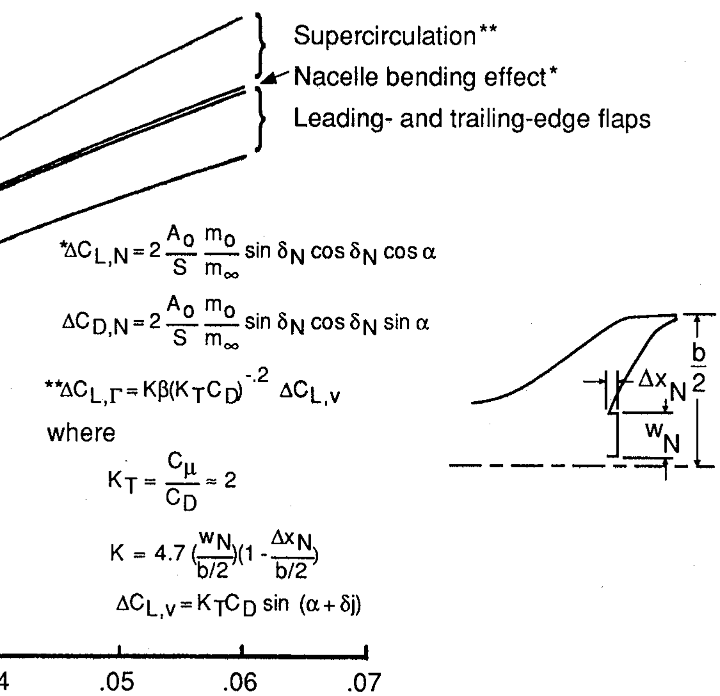

lrag at lift, $M = 0.6$, $h = 40\,000$ ft.

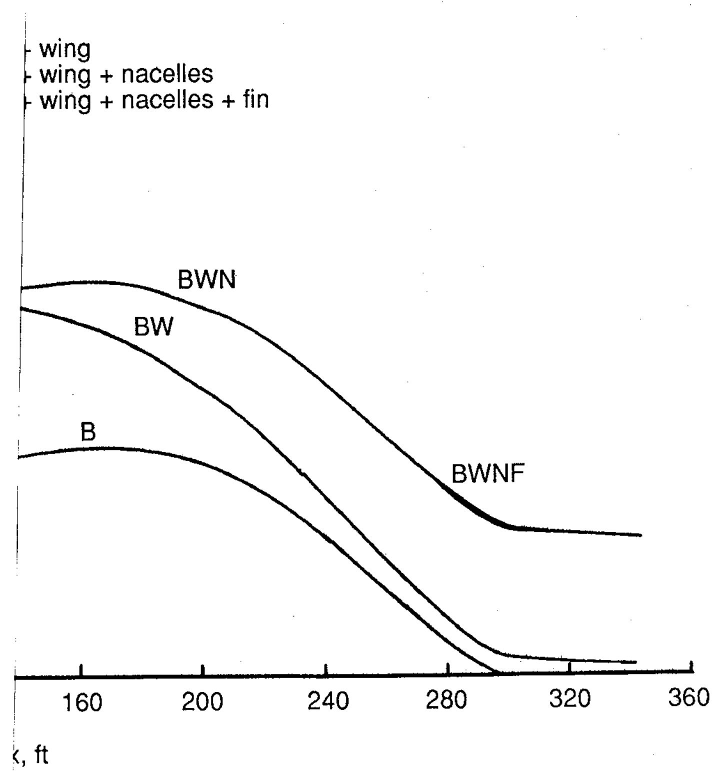

ıody area distribution at $M = 3.0$.

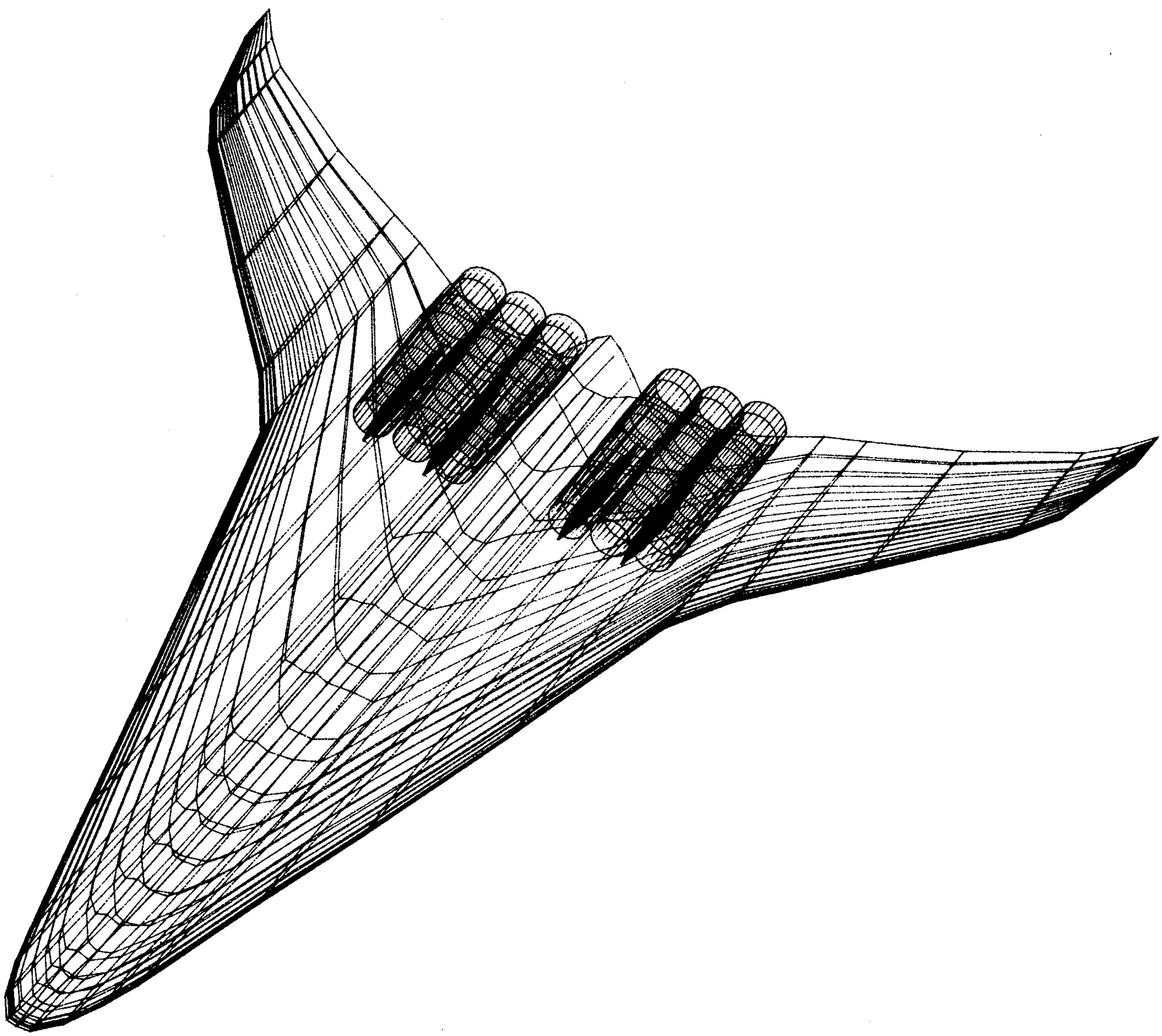

Figure 11. Numerical model for analysis at lift.

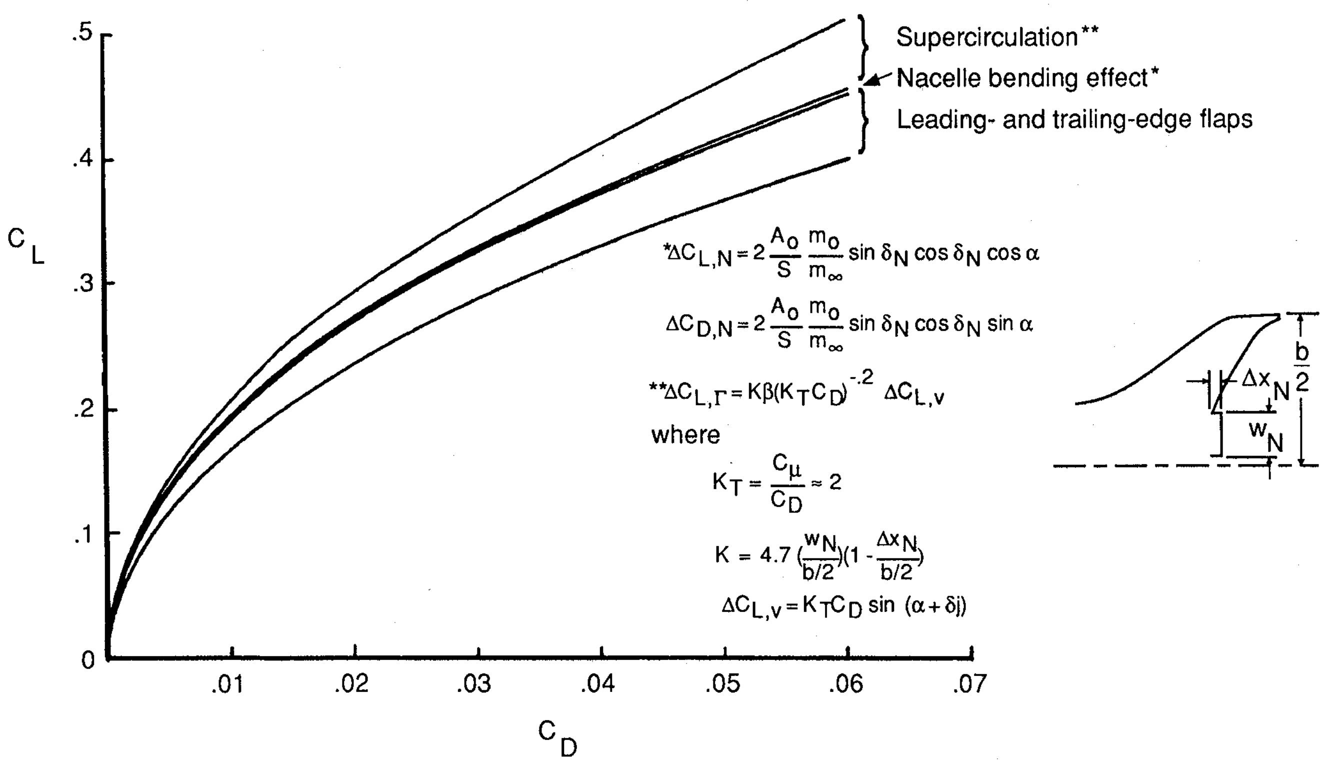

Figure 14. Buildup of drag at lift, $M = 0.6$, $h = 40\,000$ ft.

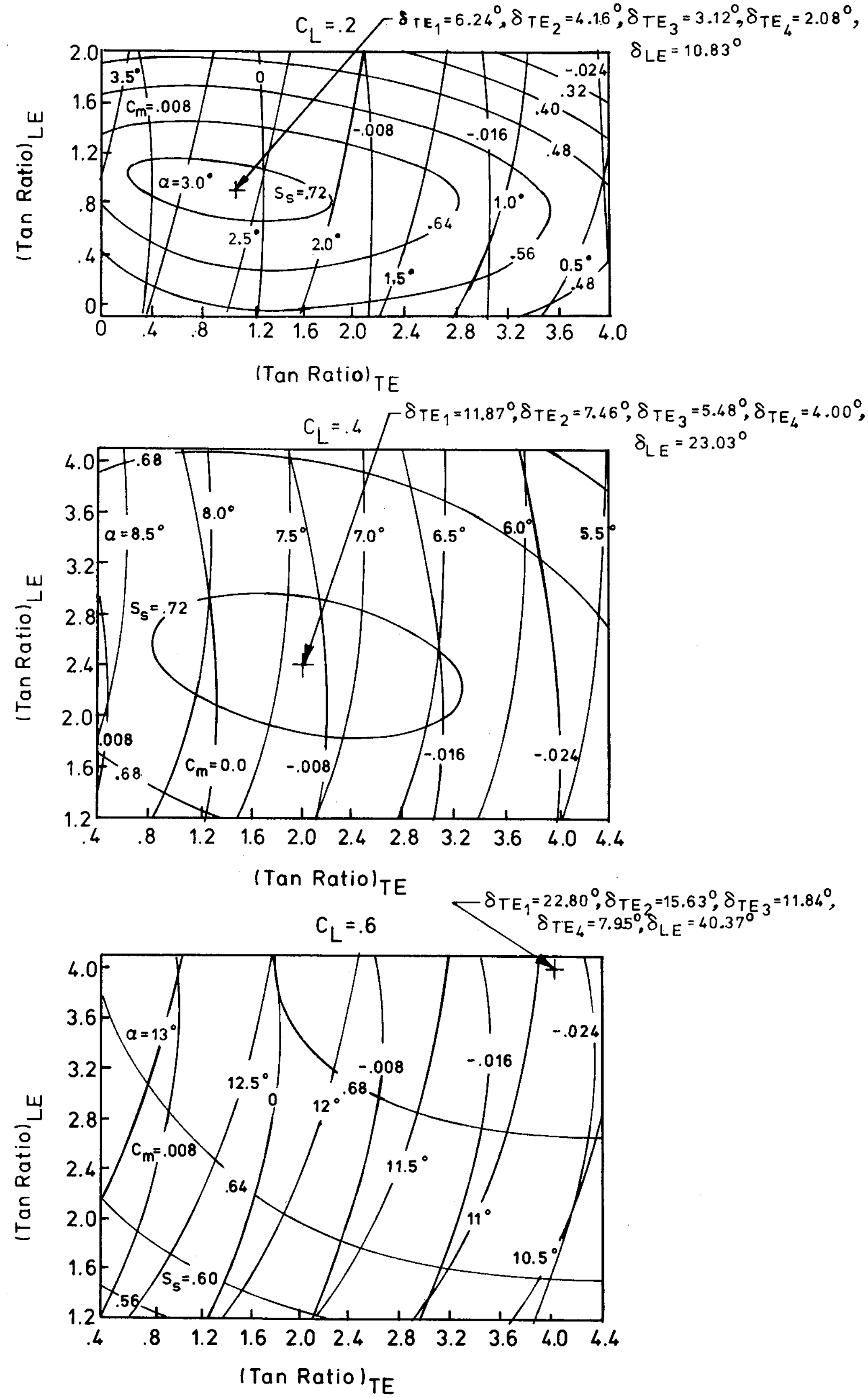

Figure 15. Flap optimization chart for $M = 0.3$, $h = 0$ ft, six-engine MRT takeoff.

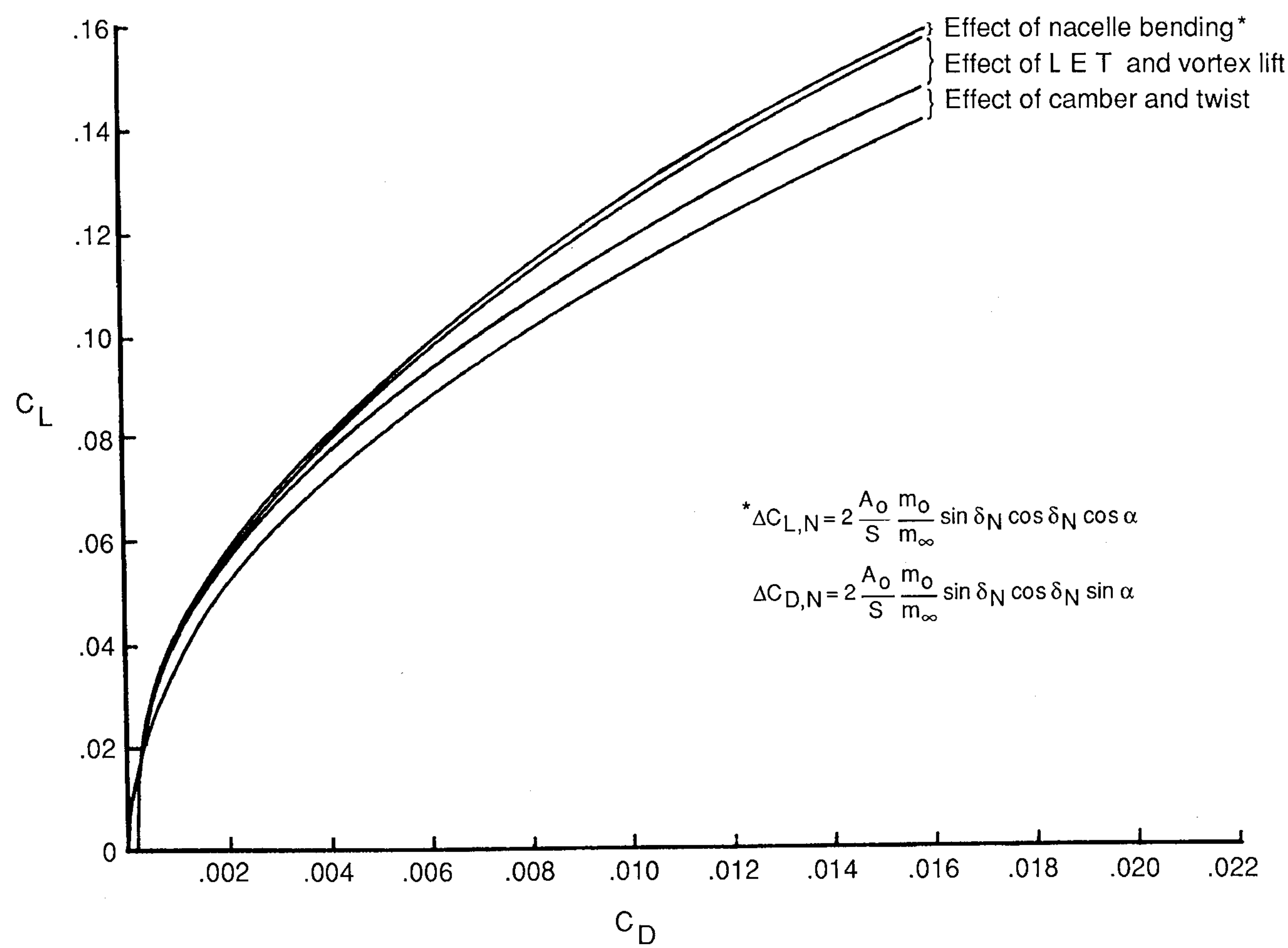

Figure 12. Lift-dependent supersonic drag buildup at $M = 3.0$.

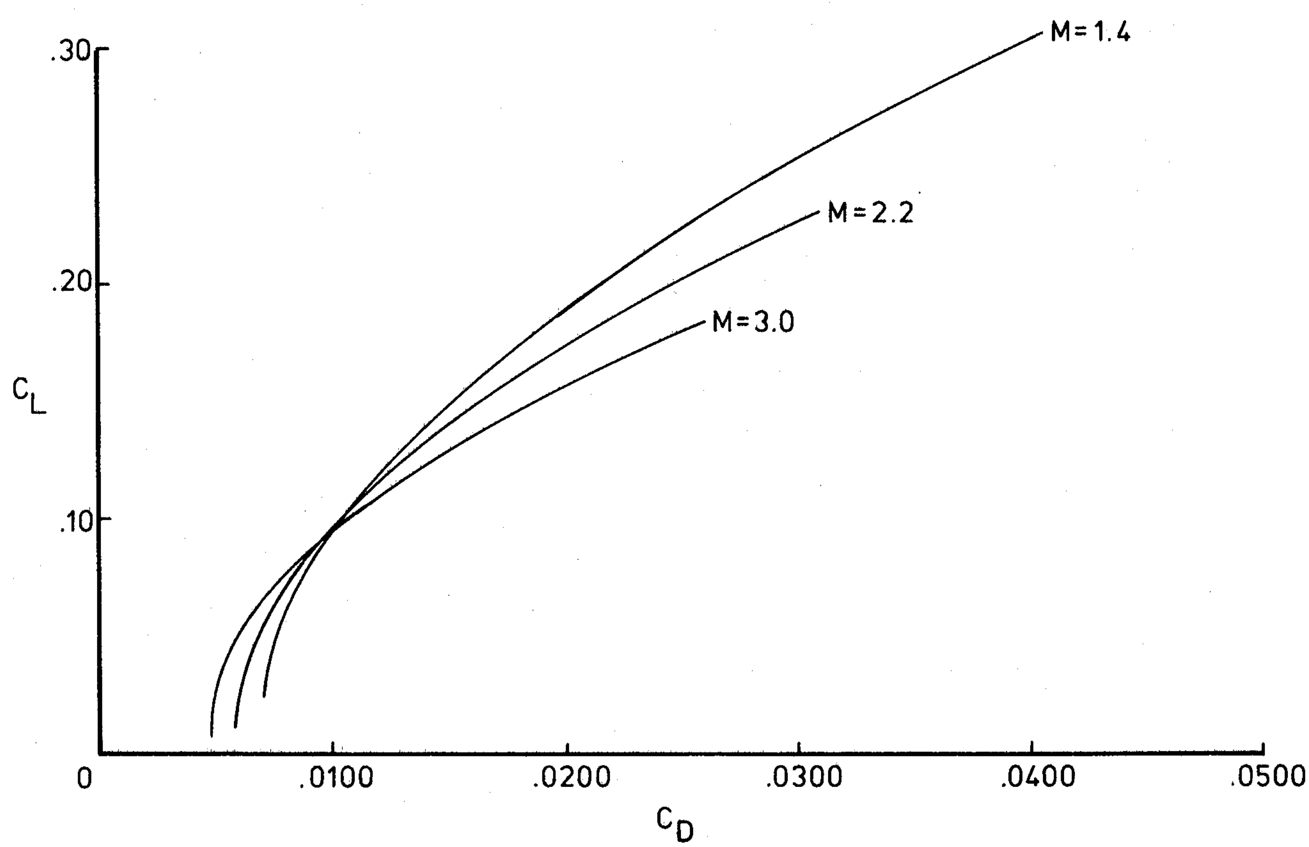

Figure 13. Drag polars for several supersonic Mach numbers, $h = 40\,000$ ft.

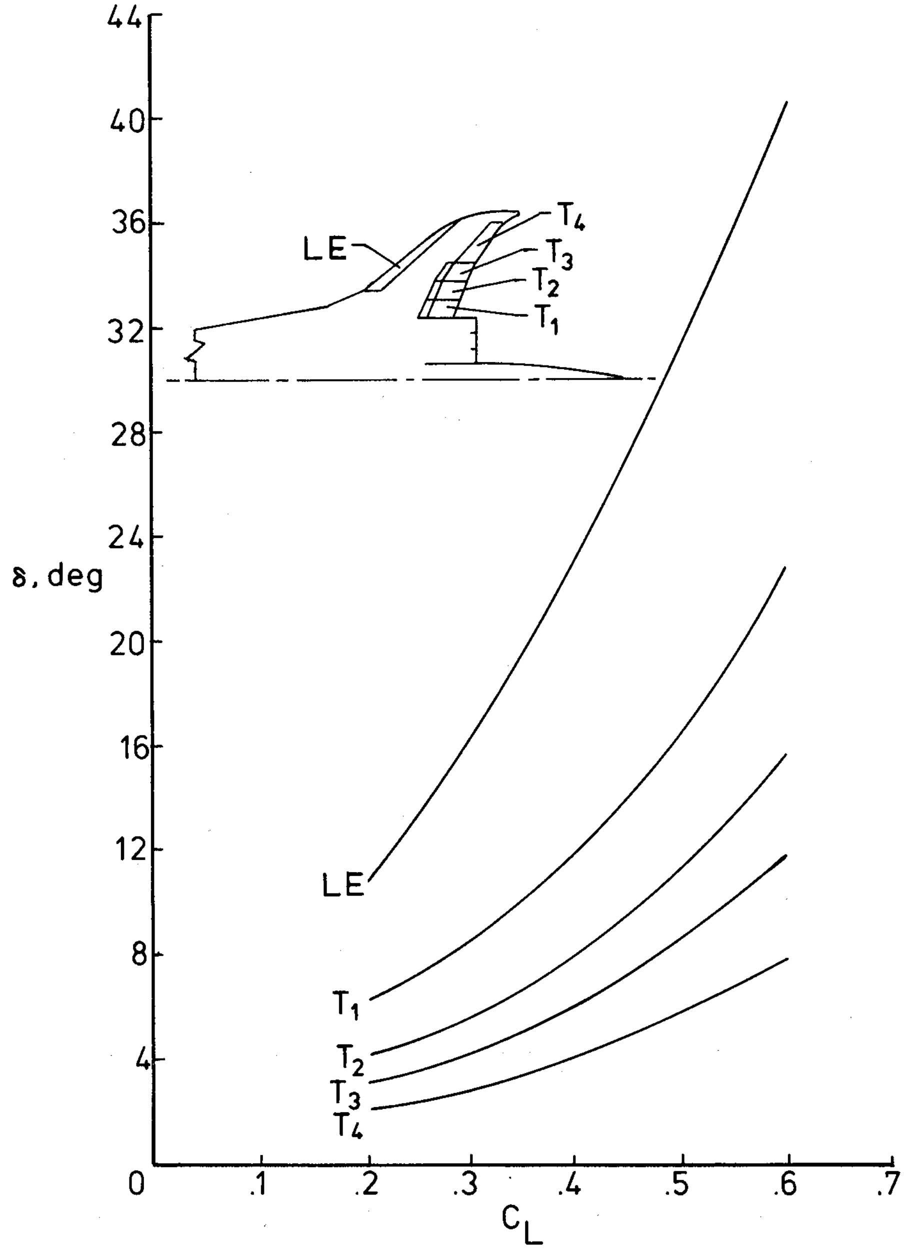

Figure 16. Optimum flap settings as a function of lift coefficient, $M = 0.3$, $h = 0$ ft, six-engine MRT takeoff.

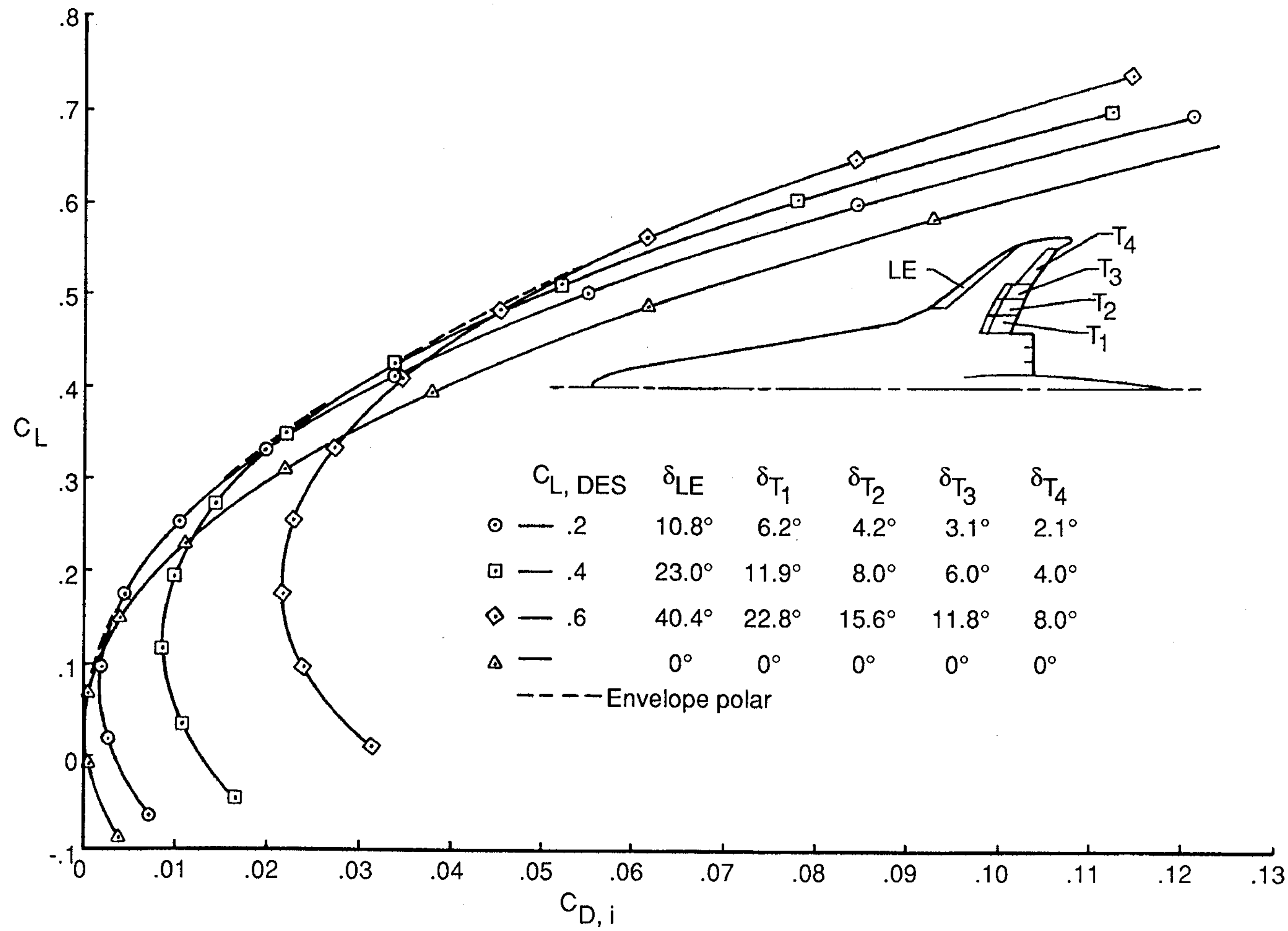

Figure 17. Generation of mission-adaptive wing (envelope) polars, $M = 0.3$, $h = 0$ ft, six-engine MRT takeoff.

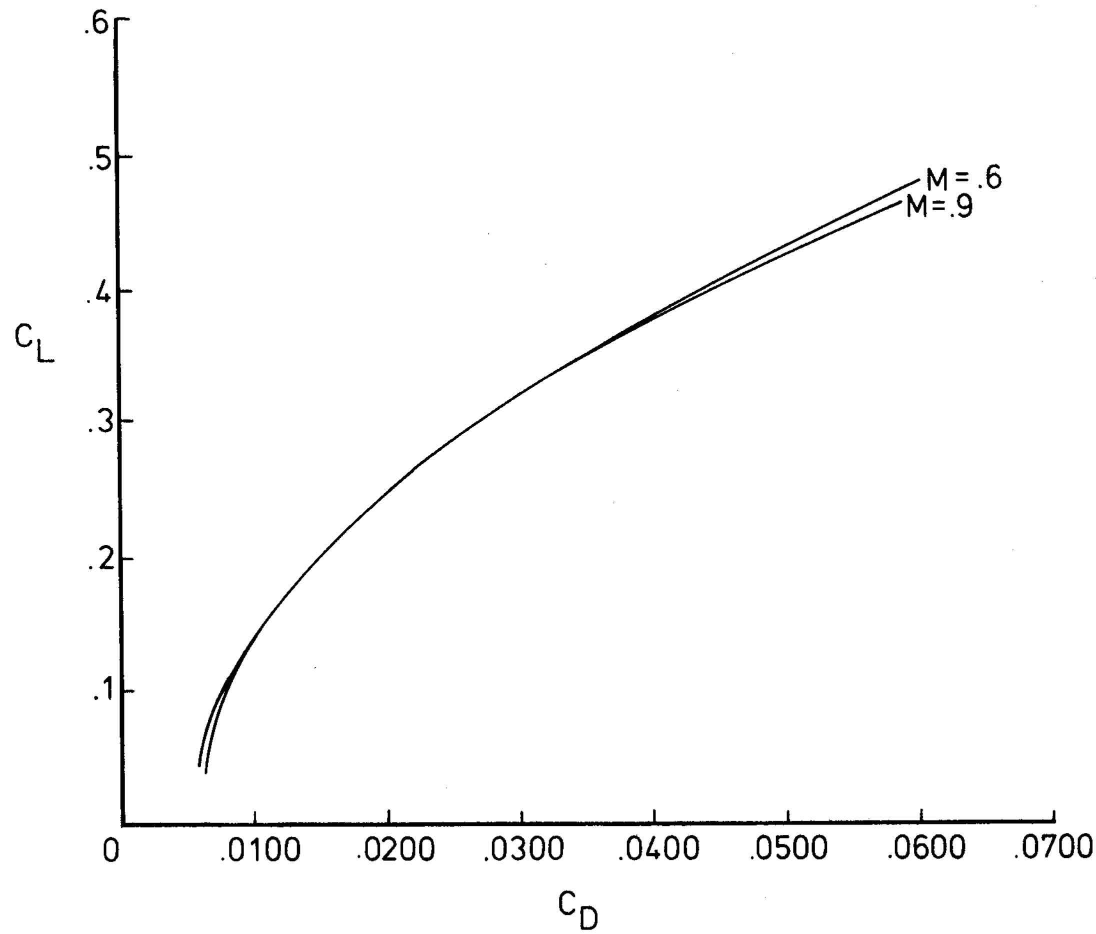

Figure 18. Subsonic polars for the mission-adaptive wing, $h = 40\,000$ ft.

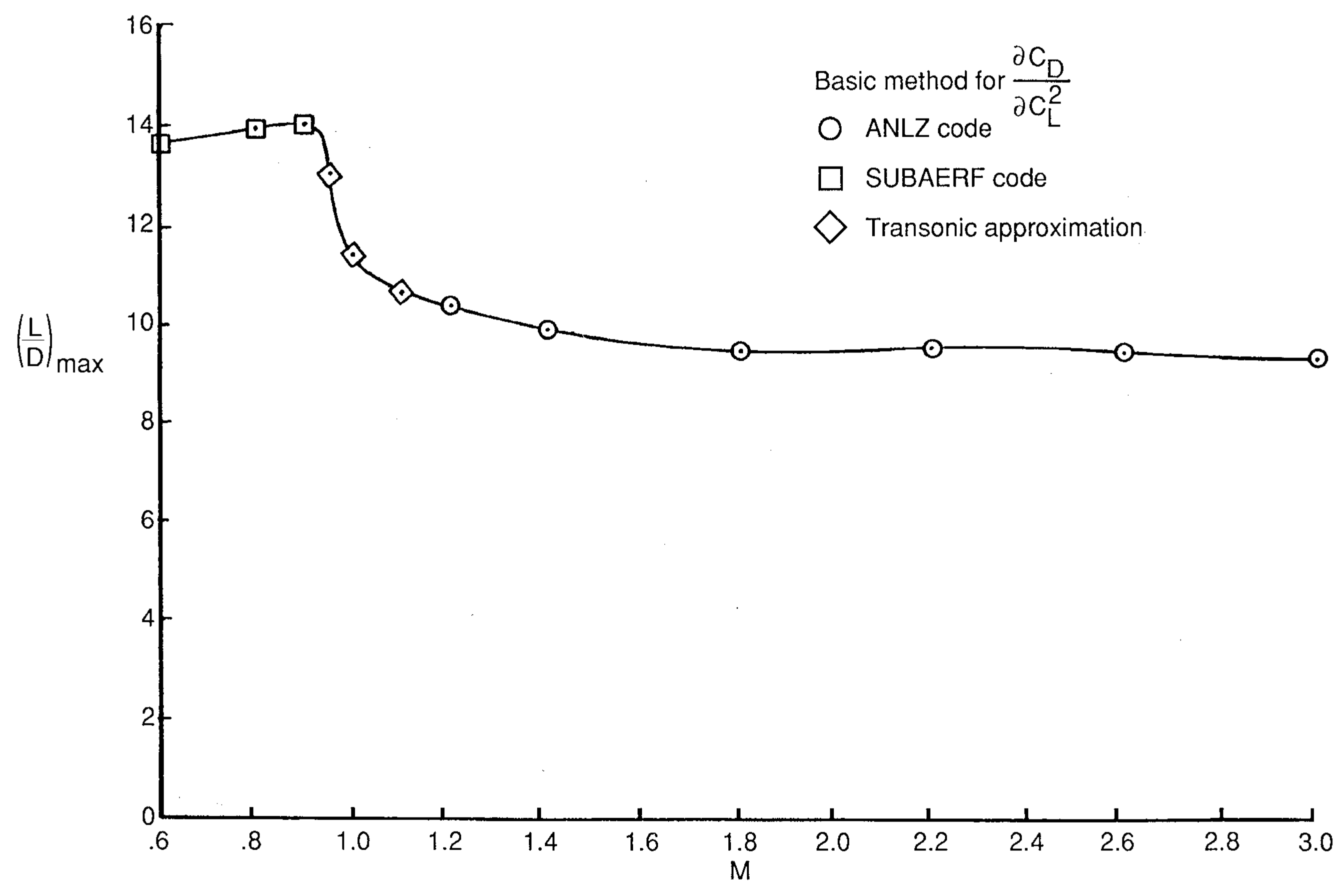

Figure 19. Maximum trimmed lift-drag ratio versus Mach number, $h = 40\,000$ ft.

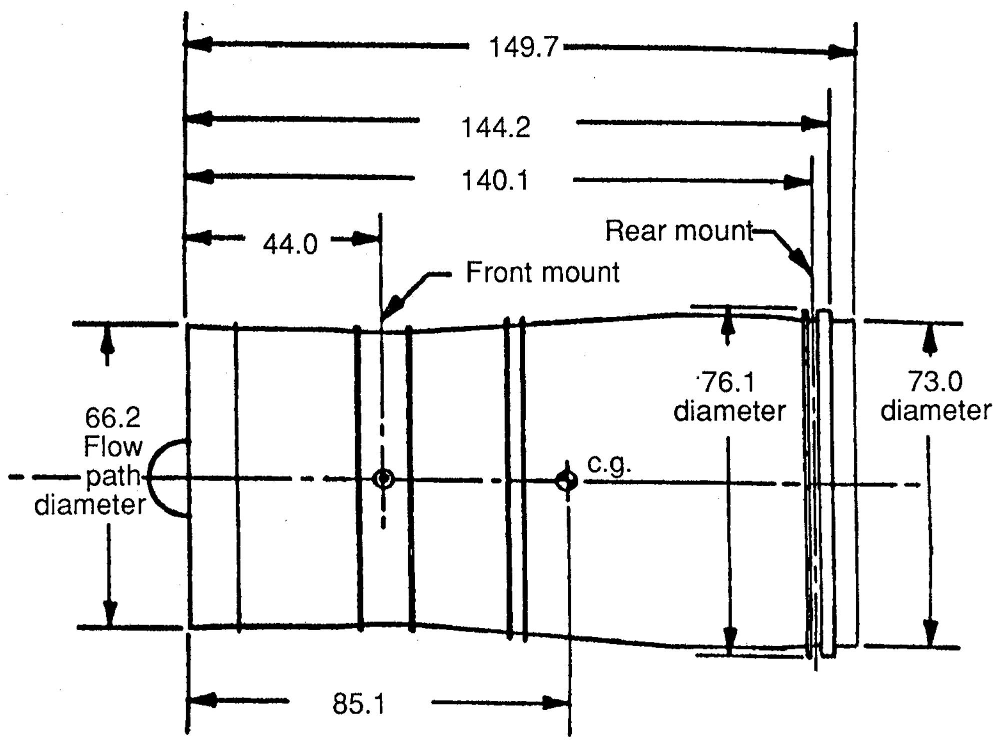

Figure 21. Engine geometry. Dimensions are in inches.

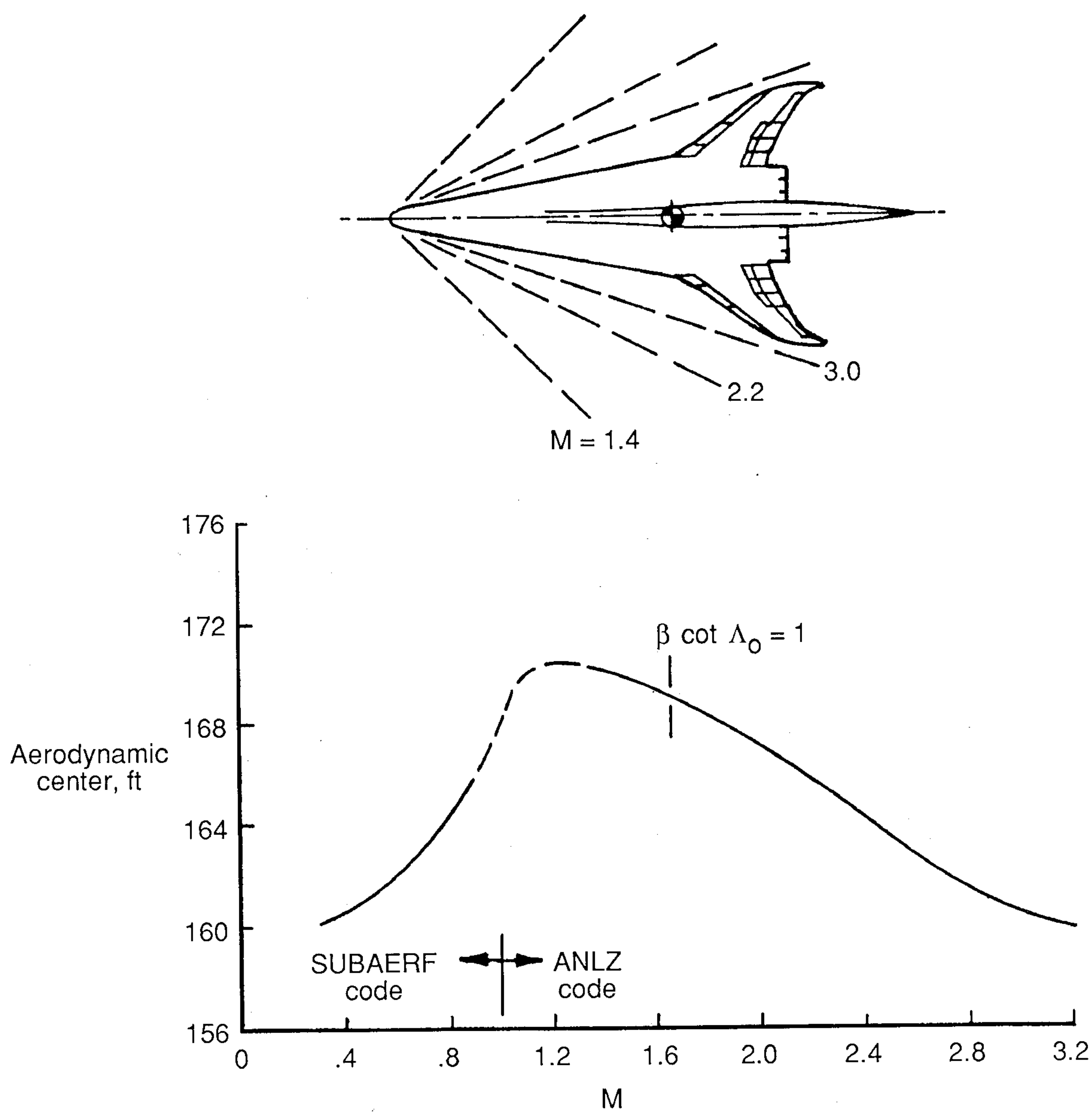

Figure 20. Aerodynamic center versus Mach number.

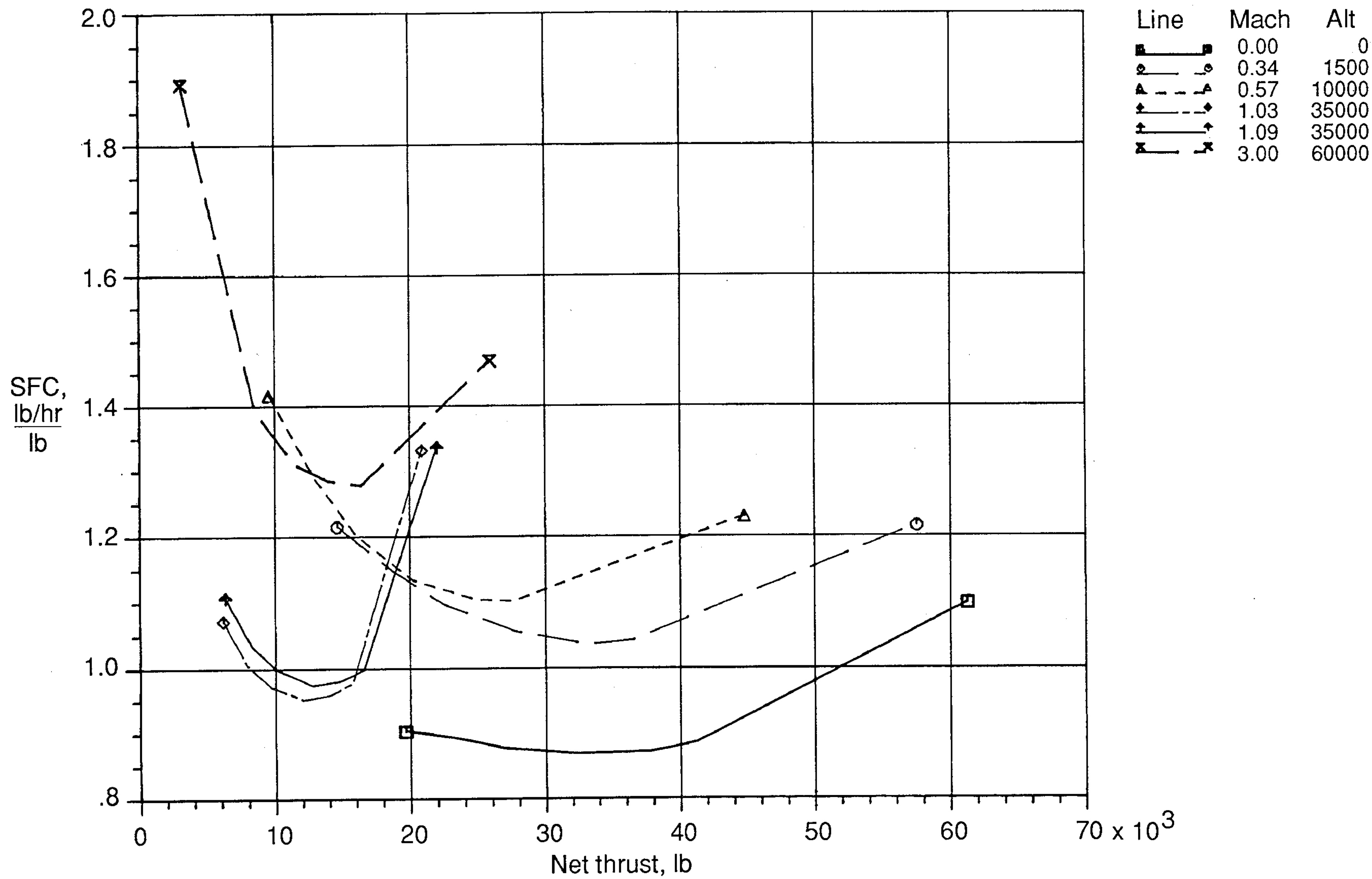

Figure 22. Engine SFC as a function of thrust.

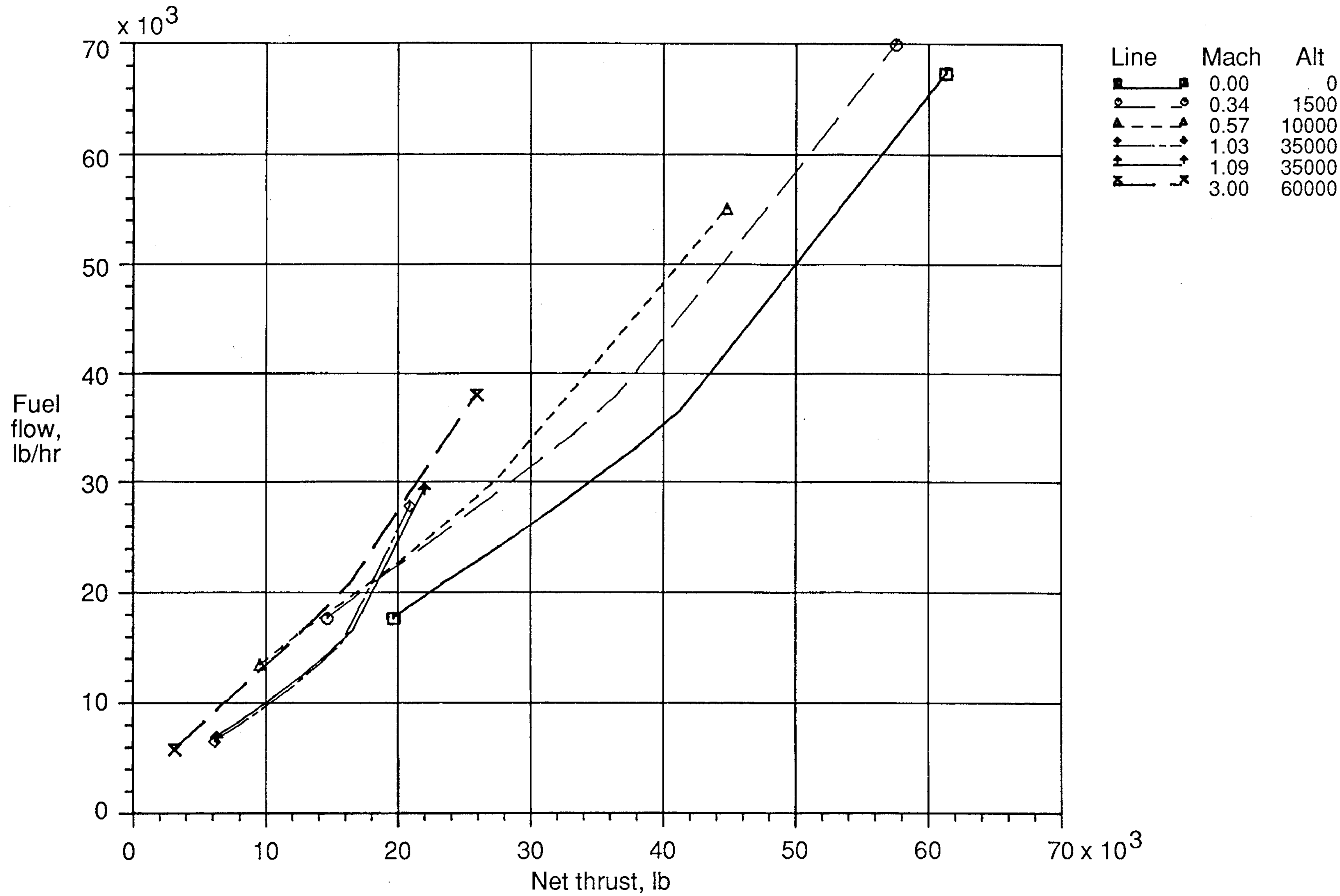

Figure 23. Engine fuel flow as a function of thrust.

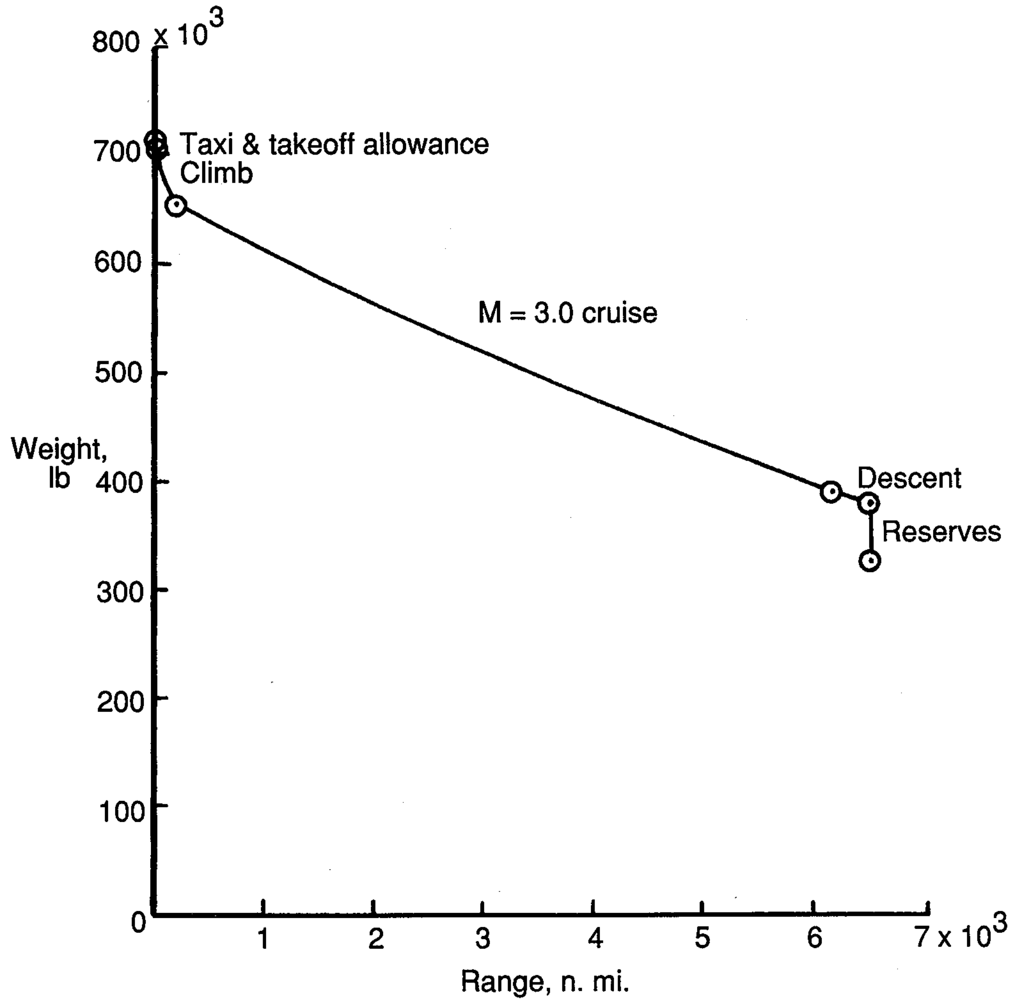

Figure 24. Design mission diagram.

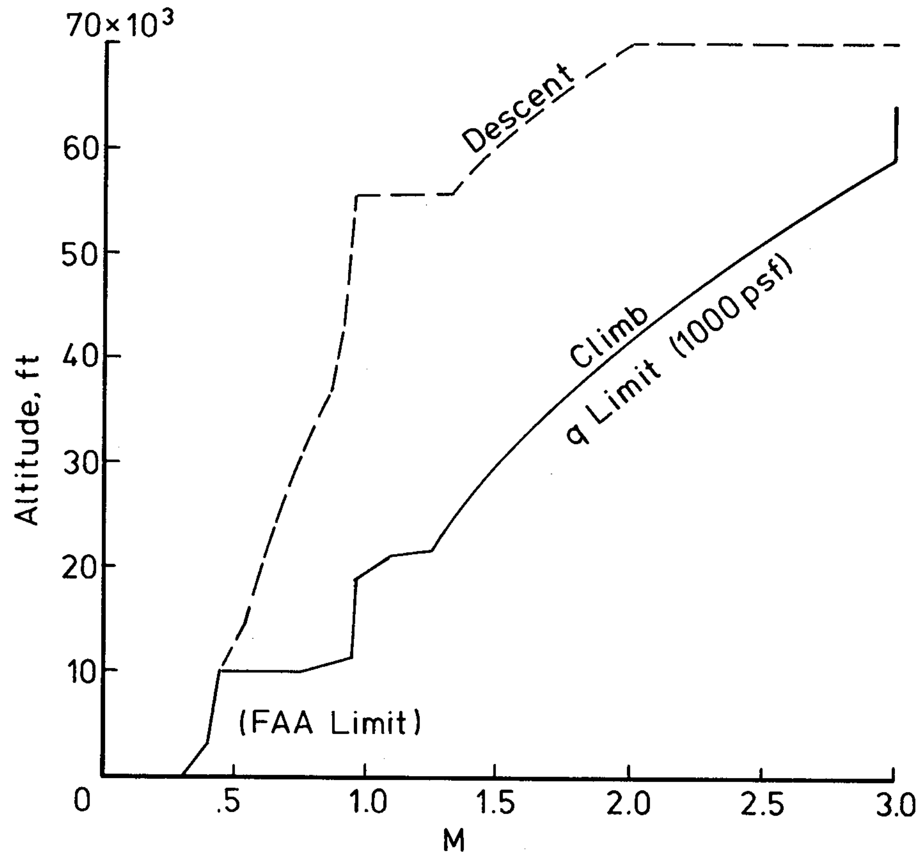

Figure 25. Climb and descent profiles.

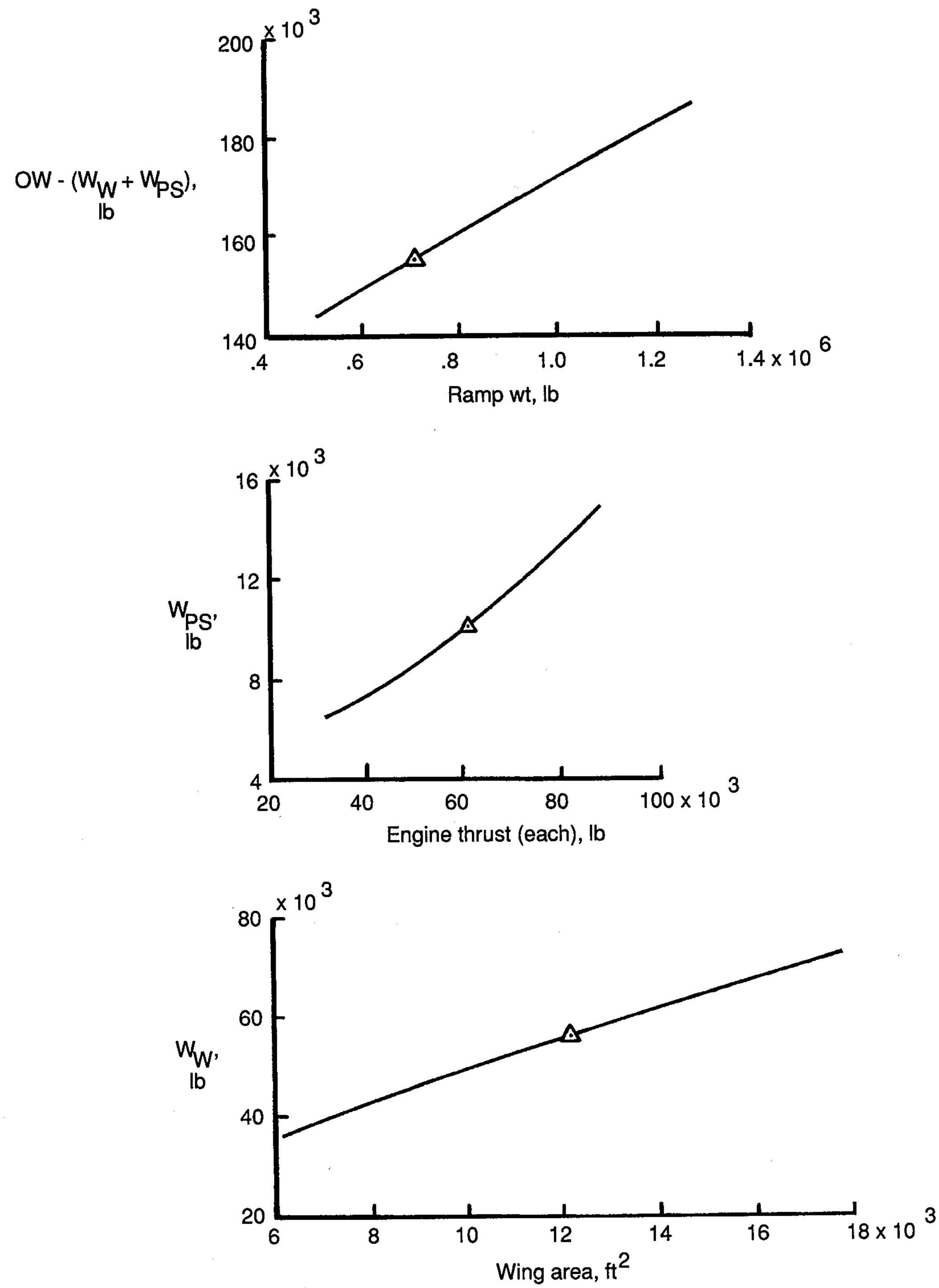

Figure 26. Trade study sensitivity data. W_W represents wing weight; W_{PS} represents propulsion system weight. Symbols denote baseline aircraft values.

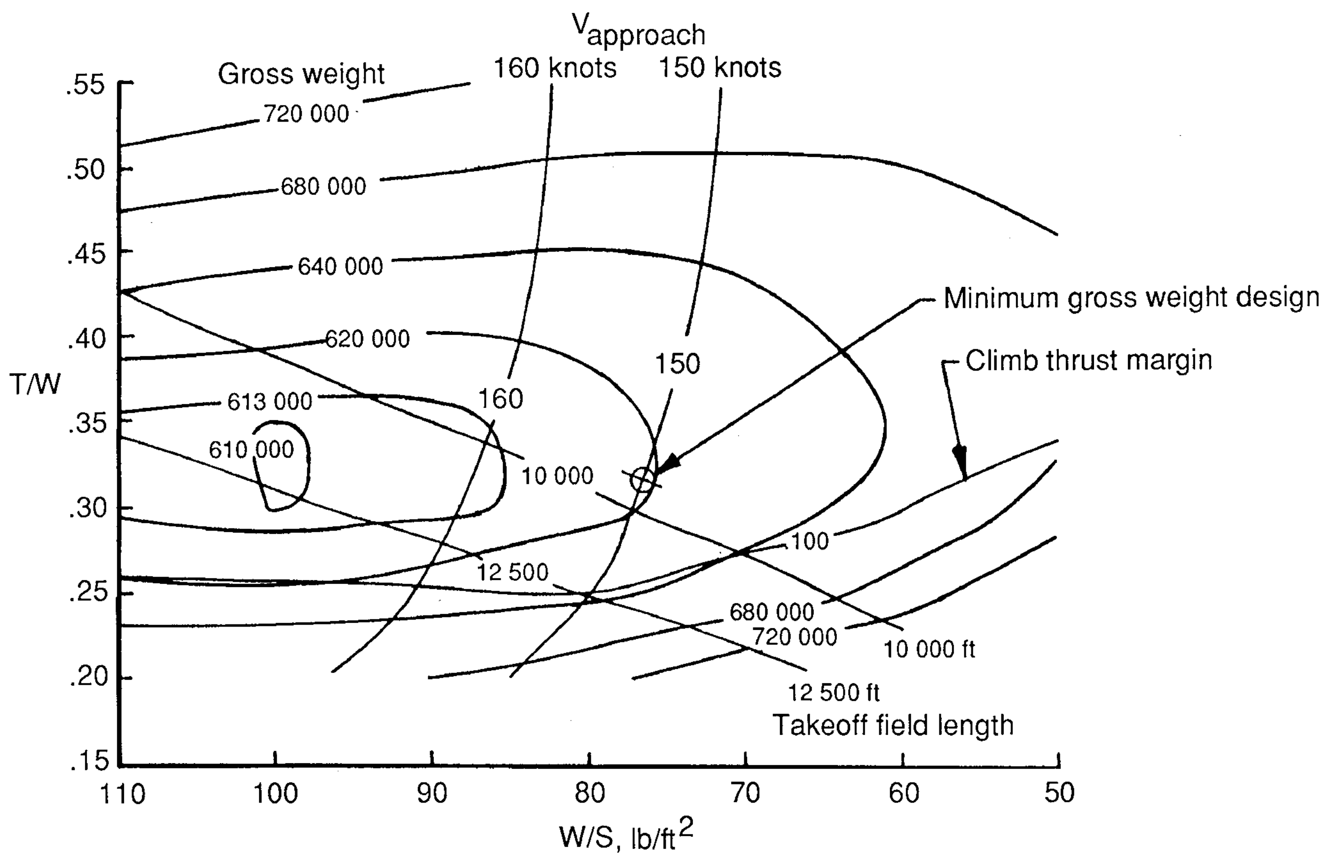

Figure 27. Gross weight as a function of thrust-weight ratio and wing loading.

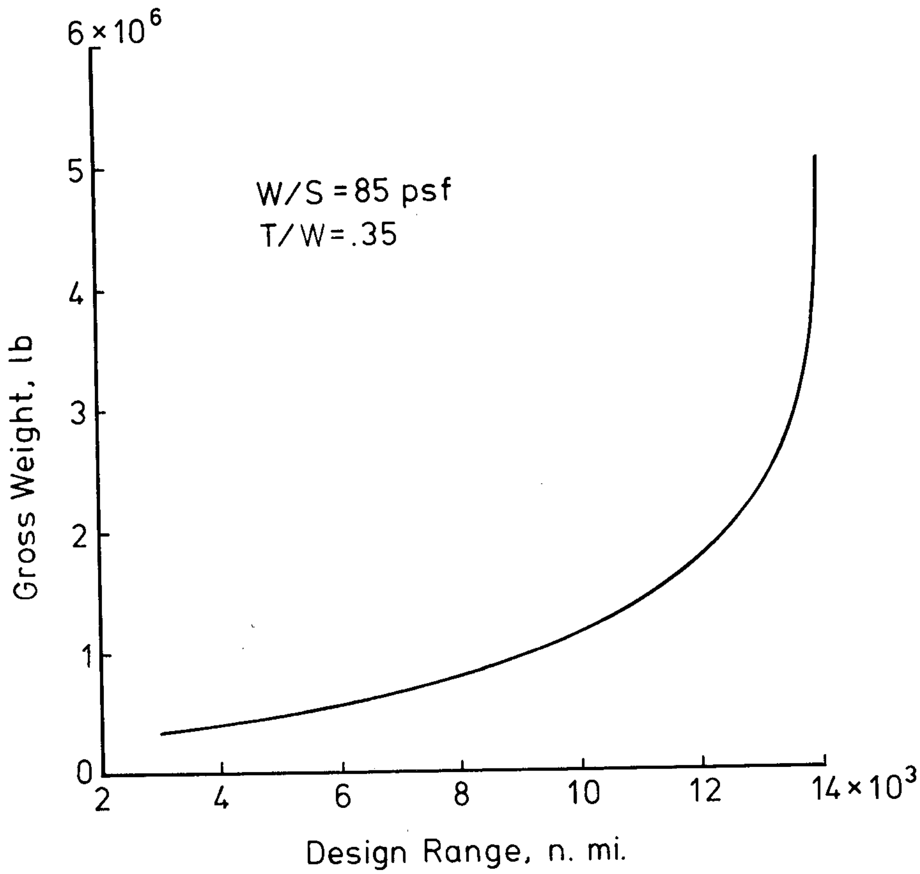

Figure 28. Gross weight as a function of range.

National Aeronautics and Space Administration

Report Documentation Page

1. Report No. NASA TM-4058	2. Government Accession No.	3. Recipient's Catalog No.
4. Title and Subtitle Concept Development of a Mach 3.0 High-Speed Civil Transport		5. Report Date September 1988
		6. Performing Organization Code
7. Author(s) A. Warner Robins, Samuel M. Dollyhigh, Fred L. Beissner, Jr., Karl Geiselhart, Glenn L. Martin, E. W. Shields, E. E. Swanson, Peter G. Coen, and Shelby J. Morris, Jr.		8. Performing Organization Report No. L-16445
9. Performing Organization Name and Address NASA Langley Research Center Hampton, VA 23665-5225		10. Work Unit No. 505-69-61-01
		11. Contract or Grant No.
12. Sponsoring Agency Name and Address National Aeronautics and Space Administration Washington, DC 20546-0001		13. Type of Report and Period Covered Technical Memorandum
		14. Sponsoring Agency Code

15. Supplementary Notes

A. Warner Robins; Fred L. Beissner, Jr.; Karl Geiselhart; Glenn L. Martin; E. W. Shields; and E. E. Swanson: Planning Research Corporation, Hampton, Virginia.
Samuel M. Dollyhigh; Peter G. Coen; and Shelby J. Morris, Jr.: Langley Research Center, Hampton, Virginia.

16. Abstract

A baseline Mach 3.0 high-speed civil transport concept was developed as part of a national program with the goal that concepts and technologies be developed that will enable an effective long-range high-speed civil transport system. The Mach 3.0 concept reported represents an aggressive application of advanced technology to achieve the design goals. The level of technology is generally considered to be that which could have a demonstrated availability date of 1995–2000. The results indicate that aircraft are technically feasible that could carry 250 passengers at Mach 3.0 cruise for a 6500-n.mi. range at a size, weight, and performance level that allow it to fit into the existing world airport structure. The details of the configuration development, aerodynamic design, propulsion system and integration, mass properties, mission performance, and sizing are presented.

17. Key Words (Suggested by Authors(s)) Supersonic cruise Aircraft design Transport aircraft		18. Distribution Statement Unclassified—Unlimited Subject Category 05	
19. Security Classif.(of this report) Unclassified	20. Security Classif.(of this page) Unclassified	21. No. of Pages 48	22. Price A03

NASA FORM 1626 OCT 86 NASA-Langley, 1988

For sale by the National Technical Information Service, Springfield, Virginia 22161-2171